Disorders can induce continuously varying universal scaling in driven systems

Astik Haldar[*] and Abhik Basu[†]

Theory Division, Saha Institute of Nuclear Physics, HBNI, Kolkata 700064, India

We elucidate the nature of universal scaling in a class of quenched disordered driven models. In particular, we explore the intriguing possibility of whether coupling with quenched disorders can lead to *continuously varying* universality classes. We examine this question in the context of the Kardar-Parisi-Zhang (KPZ) equation, with and without a conservation law, coupled with quenched disorders having distributions with pertinent structures. We show that when the disorder is relevant in the renormalization group sense, the scaling exponents can depend continuously on a dimensionless parameter that defines the disorder distribution. This result is generic and holds for quenched disorders with or without spatially long-ranged correlations, as long as the disorder remains a "relevant perturbation" on the pure system in the renormalization group sense and a dimensionless parameter naturally exists in its distribution. We speculate on its implications for generic driven systems with quenched disorders, and we compare and contrast with the scaling displayed in the presence of annealed disorders.

I. INTRODUCTION

Classification of the physics of nonequilibrium systems at long time and length scales into universality classes remains a theoretically challenging task. The standard universality classes in critical dynamics are quite robust to detailed-balance violating perturbations [1]. In contrast, genuine nonequilibrium dynamic phenomena, having non-Gibbsian steady states, are found to be rather sensitive to all kinds of perturbations. Notable examples include driven diffusive systems [2]. For instance, for the Kardar-Parisi-Zhang (KPZ) equation, anisotropic perturbations are found to be relevant in all dimensions $d \geqslant 2$ [3].

Equilibrium systems either in the vicinity of critical points or in broken symmetry phases for systems with continuous symmetries show universal scaling that depend only on the spatial dimension d and the symmetry of the order parameter (e.g., Ising, XY, nematic, etc.) [4], but they are independent of the material parameters that define the model. Prominent exceptions are the two-dimensional (2D) XY model and its related models, where the long wavelength universal properties are controlled not by a fixed point but a fixed line, and as a result, the scaling exponents of the relevant correlation functions exhibit a continuous dependence on the stiffness parameters [5]. Furthermore, equilibrium dynamics close to critical points also show dynamic universality through the dynamic scaling exponents, which characterize the time-dependence of the unequal-time correlation functions, and now may also depend upon the presence or absence of conservation laws and the nondissipative terms in the dynamical equations [6]. Genuinely nonequilibrium

systems can also show the surprising features of continuously varying nonequilibrium universal properties, which are paramatrized by dimensionless parameters that naturally appear in the formulations of the dynamical models. Well-known examples include stochastically forced fully developed three-dimensional magnetohydrodynamic turbulence [7] and stochastically coupled Burgers equations [8,9]. In all these examples, the relevant dimensionless parameters appear in the definition of the noise variances. More recently, it has been suggested that a nearly phase-ordered collection of diffusively mobile, active XY spins on a substrate can be stable, and the relevant scaling exponents that describe the phase and density correlation functions can vary continuously with certain anharmonic coupling constants that appear in the hydrodynamic equations of motion [10,11].

Disorder is known to affect the large-scale, long time universal properties of condensed matter systems. Depending upon the timescales, disorders are classified into two classes—quenched and annealed. Quenched disorders are frozen in time and do not thermalize even in equilibrium systems. In contrast, annealed disorders time-evolve and thermalize in the long time limit in equilibrium systems. Effects of quenched disorder on the universal properties of equilibrium systems are well-documented. For example, quenched disorders that locally affect the critical temperature lead to new universality classes different from the corresponding pure model; see Refs. [12–14]. Unlike quenched disorders, annealed disordered equilibrium systems may be viewed as pure systems supplemented by additional thermal degrees of freedom. This may result into different static and dynamic universality, depending upon the systems under consideration [5,15,16].

Effects of quenched disorders on nonequilibrium systems can be strikingly more complex. For instance, the random Gaussian-distributed quenched columnar disordered Kardar-Parisi-Zhang (KPZ) equation, which in one dimension (1D)

---

reduces to the periodic totally asymmetric simple exclusion process (TASEP) with short-ranged Gaussian-distributed quenched disordered hopping rates is affected by the disorder only in certain special limits of the model parameters (in 1D which is equivalent to the half-filled limit in the TASEP language), leading to new universal scaling behavior in all dimensions d. Else, pure KPZ universality holds [17,18]. In a recent study, it has been shown that the conserved KPZ (CKPZ) equation, when coupled with a particular choice of quenched disorder can modify the scaling behavior of the pure CKPZ equation in some cases [19]. Nonetheless, the question of disorder-induced continuous universality in driven models remains largely unexplored till the date.

In this article, we explore the possibility of disorder-induced continuous universality in driven models. In the absence of any general theoretical framework for nonequilibrium systems, it is useful to study simple models where such questions can be explored systematically by using analytically tractable calculations. Insights drawn from such studies should be useful to enhance general understanding of scaling in nonequilibrium setting. To that end, in this work, we have studied two models—one with a conservation law, the conserved KPZ (CKPZ) equation and the other without any conservation, the KPZ equation, both coupled with "orientational" disorders, which couples with the local gradient of the height field. By carefully choosing the disorder distributions, we show that the resulting universality classes, when they depend upon the quenched disorders, can vary continuously with a dimensionless parameter that characterizes the disorder distributions. In addition, we briefly study a version of annealed disordered CKPZ equation, and show that similar continuously varying scaling exponents can be found under certain circumstances. The remainder of the paper is organized as follows. In Sec. II, we review the pure KPZ and CKPZ universality classes. Next in Sec. III, we introduce the disordered KPZ and CKPZ equations that we use here. In Sec. IV, we elucidate the scaling properties of the quenched disordered KPZ and CKPZ equations. In Sec. V, we summarize our results. We have used one-loop dynamic renormalization group (RG) calculations for our work. We discuss some of the technical details in the Appendix for interested readers. We briefly analyze the case of annealed disordered CKPZ equation in the Appendix.

II. EQUATIONS FOR FLUCTUATING SURFACES

We consider a fluctuating surface without overhangs that may be moving (i.e., growing), on average, or not moving. Microscopically, these growth processes are described by local dynamics or local update rules and are generic examples of nonequilibrium driven systems. An interface in $d + 1$-dimensional hyperspace is characterized by variations of height $h(\mathbf{x}, t)$, where $\mathbf{x}(x_1, x_2, \ldots, x_d)$ is a position vector in the d-dimensional hypersurface. We consider fluctuating surfaces having dynamics unaffected by their absolute heights with respect to specific base planes. In other words, the dynamics is invariant under constant shifts of h. The height fluctuations display dynamic scaling [20], and the associated time-dependent correlation function in the steady states has a

scaling form

$$C(r, t - t') \equiv \langle [h(\mathbf{x}, t) - h(\mathbf{x}', t')]^2 \rangle = r^{2\chi_h} \varphi\left(\frac{r^z}{t - t'}\right) \quad (1)$$

in the long wavelength limit, where $r \equiv |\mathbf{x} - \mathbf{x}'|$; χ_h and z are *roughness exponent* and *dynamical exponent*, respectively, which classify the universality class; φ is a dimensionless scaling function. While the values of the scaling exponents are independent of the model parameters, they of course vary from one universality class to another. Two such well-known universality classes are those associated with the KPZ and CKPZ equations, which we review briefly below.

A. KPZ universality class

The KPZ equation, originally proposed as a surface growth model [21], is the paradigmatic nonequilibrium model that shows nonequilibrium phase transitions at $d > 2$. It is given by

$$\frac{\partial h}{\partial t} = \nu_1 \nabla^2 h - \frac{\lambda_1}{2}(\nabla h)^2 + \xi_h. \quad (2)$$

Here, $\nu_1 > 0$ is a diffusivity, and λ_1 is a nonlinear coefficient. Furthermore, ξ_h is noise with Gaussian distribution and zero mean, that is added to describe the inherent stochasticity of the dynamics. It is a white noise, since h in Eq. (2) obeys a nonconserved dynamics. Stochastic noise ξ_h has a variance

$$\langle \xi_h(\mathbf{x}, t) \xi_h(\mathbf{x}', t') \rangle = 2D_1 \delta^d(\mathbf{x} - \mathbf{x}') \delta(t - t'), \quad (3)$$

where $D_1 > 0$ is the noise strength. In addition to its application as a surface growth model, Eq. (2) serves as the active or nonequilibrium hydrodynamic model for a smoothly varying phase, when there is no other hydrodynamic variable present [22], and an *active fluid membrane* without momentum conservation [23].

Equation (2) is invariant under the transformation $\mathbf{x} \rightarrow \mathbf{x} - \lambda_1 \mathbf{a}t$, $t \rightarrow t$, $h \rightarrow h + \mathbf{a} \cdot \mathbf{x} + \frac{\lambda_1}{2}|\mathbf{a}|^2 t$, known as the tilt invariance [20]. This in turn gives an exact exponent relation $\chi_h + z = 2$ [20,24]. In 1D the scaling exponents are found exactly as a consequence of the tilt invariance (that holds at all dimensions) and the Fluctuation-Dissipation-Theorem that holds only at 1D [20]. This gives dynamic exponent $z = 1/2$ and roughening exponent $\chi_h = 3/2$ *exactly*, corresponding to a 1D rough surface. In 2D, which is the *lower critical dimension* of this model, there is only a "rough" phase which is perturbatively inaccessible. Furthermore, the KPZ equation has smooth phase above 2D for low enough noise, the scaling property of which is identical to the linear Edward-Wilkinson (EW) equation [20] with $z = 2$, $\chi_h = \frac{2-d}{2}$. As the noise strength is increased, the KPZ equation undergoes a phase transition from a smooth to a perturbatively inaccessible rough phase in dimension $d > 2$.

B. CKPZ universality class

The CKPZ equation, which is essentially the conserved analog of the KPZ equation, forms a universality class distinct from the KPZ equation. This of course is not surprising, since in nonequilibrium systems, the presence or absence of conservation laws not only affect the dynamic scaling exponents, they can in principle affect the static exponents

(e.g., the roughness exponent) as well, in contrast to equilibrium systems. In the CKPZ equation, the height field $h(\mathbf{x}, \mathbf{t})$ of an interface of a volume conserving system, a single-valued function measured with respect to an arbitrary base plane, follows a generic conservation laws:

$$\partial_t h = -\nabla \cdot \mathbf{J}, \tag{4}$$

where $\mathbf{J}$, the current, has the following form [25]:

$$\mathbf{J} = \nabla \left[\nu_2 \nabla^2 h - \frac{\lambda_2}{2} (\nabla h)^2 \right]. \tag{5}$$

We note that current $\mathbf{J}$ in Eq. (5) is constructed in such a way that $\mathbf{J}(\mathbf{k} = \mathbf{0}, t) = 0$, where $\mathbf{k}$ is a wave vector. With this, the CKPZ equation takes the form [25]

$$\frac{\partial h}{\partial t} = -\nabla^2 \left[\nu_2 \nabla^2 h - \frac{\lambda_2}{2} (\nabla h)^2 \right] + \eta_h. \tag{6}$$

Here, η_h is a conserved noise that models stochastic nature of dynamics. It is assumed to be zero-mean and Gaussian distributed with a variance

$$\langle \eta_h(\mathbf{x}, t) \eta_h(\mathbf{x}', t') \rangle = 2D_2(-\nabla^2) \delta^d(\mathbf{x} - \mathbf{x}') \delta(t - t'). \tag{7}$$

In the linear limit, i.e., with $\lambda_2 = 0$, Eq. (6) reduces to the Mullins-Herring (MH) equation for linear MBE processes [26,27]. Equation (6) is not tilt invariant, and hence, it has no exact exponent relation in contrast to the KPZ equation [28]. Results from one-loop RG study shows that $d = 2$ is the upper critical dimension, and below 2D, in an $\epsilon = 2 - d$ expansion one finds the scaling exponents as $z = 4 - \frac{\epsilon}{3}$, $\chi_h = \frac{\epsilon}{3}$. This corresponds to a rough phase. At 2D the interface is *logarithmically* rough and above 2D, the surface is smooth, with long wavelength scaling properties statistically identical to those obtained from the linear MH equation. Unlike the KPZ equatiom, the CKPZ equation does not admit a smooth-to-rough transition for strong coupling.[1]

III. DISORDERED KPZ AND CKPZ EQUATIONS

We now minimally couple the KPZ Eq. (2) and CKPZ Eq. (6) equations with "orientational" quenched disorder to address the question on universality we raised above. We call it an orientational disorder, since it, a random quenched disordered vector field $\mathbf{V}(\mathbf{x})$, whose statistics is given below, couples with the fluctuation in the local orientation of the height field given by ∇h. Further, V_i can in general have both irrotational and solenoidal parts. Quenched vector V_i is assumed to be zero-mean, Gaussian-distributed with a variance

$$\langle V_i(\mathbf{x}) V_j(\mathbf{x}') \rangle = [2D_T P_{ij} + 2D_L Q_{ij}] |\mathbf{x} - \mathbf{x}'|^{-\alpha}. \tag{8}$$

Here P_{ij} and Q_{ij} are the transverse (solenoidal) and longitudinal (irrotational) projection operators, respectively. In the

---

[1]A generalized CKPZ equation has recently been proposed that contains an additional nonlinear term which is as relevant (in a RG sense) as the existing nonlinear term in Eq. (6). This admits a roughening transition; see F. Caballero *et al.*, Strong coupling in conserved surface roughening: A new universality class? Phys. Rev. Lett. **121**, 020601 (2018). We do not discuss that here.

Fourier space, these are given by

$$P_{ij}(\mathbf{k}) = \delta_{ij} - \frac{k_i k_j}{k^2}, \quad Q_{ij}(\mathbf{k}) = \frac{k_i k_j}{k^2}. \tag{9}$$

Thus, $P_{ij}(\mathbf{k})$ and $Q_{ij}(\mathbf{k})$, respectively, project any vector they operate on to directions normal and parallel to $\mathbf{k}$. Evidently at 1D, $P_{ij} \equiv 0$ identically. Noise strengths D_T and D_L are positive definite. The exponent α paramatrises the measure of how *long range* or how spatially correlated the quenched disorder is; we take $0 \leqslant \alpha < d$ (in this range the short distance cutoff implied in the Fourier transforms can be smoothly taken to zero). In the Fourier space the disorder correlation Eq. (8) takes the form

$$\langle V_i(\mathbf{k}, \omega) V_j(\mathbf{k}', \omega') \rangle = [2D_T P_{ij} + 2D_L Q_{ij}] k^{-\mu}$$
$$\times \delta^d(\mathbf{k} + \mathbf{k}') \delta(\omega') \delta(\omega), \tag{10}$$

where $\mu \equiv d - \alpha > 0$ for spatially long-ranged correlated disorders. In the more familiar short-ranged disorder case,

$$\langle V_i(\mathbf{x}) V_j(\mathbf{x}') \rangle = [2D_T P_{ij} + 2D_L Q_{ij}] \delta^d(\mathbf{x} - \mathbf{x}') \tag{11}$$

in real space. In the Fourier space, this gives Eq. (10) with $\mu = 0$. Clearly, when $D_L = D_T$, the rhs of Eq. (11) is proportional to δ_{ij} [19]. Further, in the extreme limits when $D_T = 0$, the quenched vector field $\mathbf{V}$ is irrotational, whereas for $D_L = 0$, it is solenoidal.

In the next Sections, we study the effects of the coupling of V_i with the KPZ and CKPZ equations, and explore their universal scaling properties, in particular, the dependence on the dimensionless ratio $\gamma \equiv D_T/D_L$.

A. KPZ equation with quenched disorder

Given the status of the KPZ equation as a paradigmatic nonequilibrium model that shows phase transitions, it is of great theoretical interest to study whether or not quenched disorder can modify the universality classes of the pure system. The quenched disordered version of the KPZ equation—the KPZ equation with minimally coupled orientational quenched disorder that we use is

$$\frac{\partial h}{\partial t} = \nu_1 \nabla^2 h - \frac{\lambda_1}{2} (\nabla h)^2 + \kappa_1 (\mathbf{V} \cdot \nabla h) + \xi_h. \tag{12}$$

The disorder-dependent nonlinear term with coefficient κ_1 is the leading order nonlinear term that respects the invariance under a constant shift of h (see Ref. [29] for a similar coupling). It breaks the tilt invariance of the pure KPZ equation. As a result, Eq. (12) lacks any exact exponent identity, in direct contrast with the pure KPZ equation. Further, the sign of κ_1 is arbitrary. Equation (12) reduces to the pure KPZ Eq. (2) for $\kappa_1 = 0$. The additive annealed noise ξ_h is assumed to be zero-mean, Gaussian-distributed with a variance given by Eq. (3). Just as the pure KPZ Eq. (2) is the nonequilibrium hydrodynamic model of a phase in the absence of any other hydrodynamic variables, Eq. (12) is the nonequilibrium hydrodynamic model of a smoothly varying phase field in the presence of orientational quenched disorder in the absence of any other hydrodynamic variables, or of an active fluid membrane with quenched disorder with broken tilt invariance and without momentum conservation. Thus, this study should

provide insight to the role of quenched disorders in these systems.

B. CKPZ equation with quenched disorder

To study the CKPZ equation minimally coupled with orientational quenched disorder, we use the disordered version of the CKPZ equation proposed and studied in Ref. [19]. The form of the current **J** corresponding to this disordered CKPZ equation reads

$$\mathbf{J} = \boldsymbol{\nabla} \left[\nu_2 \nabla^2 h - \frac{\lambda_2}{2} (\boldsymbol{\nabla} h)^2 - \kappa_2 (V \cdot \boldsymbol{\nabla} h) \right]. \quad (13)$$

The coefficient κ_2 is the coupling constant of the disorder-dependent leading order nonlinear term that respects the invariance under a constant shift of h; κ_2 can take any sign. The choice of disorder coupling that current $\mathbf{J}(\mathbf{k} \to 0, t) \to 0$ at the thermodynamic limit. With $\kappa_2 = 0$, the model reduces to the pure CKPZ Eq. (6). With Eq. (13), the disordered CKPZ equation reads

$$\partial_t h = \nabla^2 \left[-\nu_2 \nabla^2 h + \frac{\lambda_2}{2} (\boldsymbol{\nabla} h)^2 + \kappa_2 (V \cdot \boldsymbol{\nabla} h) \right] + \eta_h. \quad (14)$$

The noise η_h satisfy the same as Eq. (7).

In the next section we analyze the scaling properties of these disordered models.

IV. UNIVERSAL SCALING IN THE DISORDERED MODELS

The universality classes of the pure KPZ and CKPZ equations are well-established. We now set out to find whether the quenched disorder is a relevant perturbation on these universality classes, and if so, what the new universality classes are. The nonlinear terms present in Eqs. (12) and (14) preclude any exact analysis of the problem, and necessitate use of perturbative approaches. The naïve perturbation theory produces diverging corrections to the model parameters in the long wavelength limit. We use here the dynamic RG framework to systematically handle these diverging corrections in the long wavelength limit. We outline this method below. It is convenient to express the stochastically driven Eqs. (12) and (14) as path integrals over configurations of $h(\mathbf{r}, t)$ and its dynamic conjugate field $\hat{h}(\mathbf{r}, t)$ [30,31], subject to the distribution of the quenched disorders as specified above. The momentum shell RG procedure consists of integrating over the short wavelength Fourier modes of $h(\mathbf{r}, t)$, $\hat{h}(\mathbf{r}, t)$, and $V_i(\mathbf{r})$, followed by rescaling of lengths and times [31]. In particular, we follow the usual convention of initially restricting the wave vectors to be within a bounded spherical Brillouin zone: $|\mathbf{k}| < \Lambda$. However, the precise value of the upper cutoff Λ has no effect on our final results. The fields $h(\mathbf{r}, t)$, $\hat{h}(\mathbf{r}, t)$, and $V_i(\mathbf{r})$ are separated into the high and low wave-vector parts $h(\mathbf{r}, t) = h^<(\mathbf{r}, t) + h^>(\mathbf{r}, t)$, $\hat{h}(\mathbf{r}, t) = \hat{h}^<(\mathbf{r}, t) + \hat{h}^>(\mathbf{r}, t)$, and $V_i(\mathbf{r}) = V_i^<(\mathbf{r}) + V_i^>(\mathbf{r})$, where $h^>(\mathbf{r}, t)$, $\hat{h}^>(\mathbf{r}, t)$, and $V_i(\mathbf{r})^>$ have support in the large wave-vector (short wavelength) range $\Lambda e^{-l} < |\mathbf{k}| < \Lambda$, while $h^<(\mathbf{r}, t)$, $\hat{h}^<(\mathbf{r}, t)$, and $V_i^<(\mathbf{r})$ have support in the small wave-vector (long-wavelength) range $|\mathbf{k}| < e^{-l}\Lambda$; $b \equiv e^l > 1$. We then integrate out $h^>(\mathbf{r}, t)$, $\hat{h}^>(\mathbf{r}, t)$, and $V_i^>(\mathbf{r})$

perturbatively in the anharmonic couplings, which can only be done perturbatively; as usual, this resulting perturbation theory of $h^<(\mathbf{r}, t)$, $\hat{h}^<(\mathbf{r}, t)$, and $V_i^<(\mathbf{r})$ can be represented by Feynman graphs, with the order of perturbation theory reflected by the number of loops in the graphs we consider; see, e.g., Refs. [17,18]. This procedure allows us to calculate the RG flow equations which give the stable fixed points of the disordered KPZ and CKPZ equations, which in turn give the associated scaling exponents. In the next Sections, we analyze the RG flow equations and elucidate the scaling exponents for the quenched disordered KPZ and CKPZ equations separately. Interested readers will find the relevant one-loop Feynman diagrams and other details of the intermediate steps in Appendix C.

A. Quenched disordered KPZ equation

The dynamic exponent and roughness exponent in the linear limit of Eq. (12) are $z = 2$ and $\chi_h = \frac{2-d}{2}$, respectively, which are unsurprisingly identical to their values in the linear limit of the pure KPZ equation; see also Appendix B 1. We now study the effects of nonlinear terms on long time and long wavelength scaling behavior of the linear theory by using one-loop perturbative RG methods, whose basic steps are outlined above.

We define dimensionless effective coupling constants $g_1 = \frac{\lambda_1^2 D_1}{\nu^3} \tilde{K}_d$, $g_2 = \frac{\kappa_1^2 D_T}{\nu_1^2} \tilde{K}_d$ and $g_3 = \frac{\kappa_1^2 D_L}{\nu_1^2} \tilde{K}_d$, where $\tilde{K}_d = \frac{\int d\Omega_d}{(2\pi)^d}$ contains the angular contribution coming from the d-dimensional volume integral. There are no fluctuation corrections to D_L and D_T. Under rescaling of space and time, we rescale the fields in such a way that D_L and D_T do not scale. The ratio $\gamma = \frac{D_T}{D_L} \equiv \frac{g_2}{g_3}$ is marginal in this theory, as we shall see below. Therefore, we do not need to separately study the RG flows of g_2 and g_3; solving anyone of them suffices, as the other can be eliminated in terms of γ. For convenience we choose to work with g_1 and g_3. Under the rescaling of space, time and the fields as given in Appendix C 2, effective coupling g_1 scales as $\exp[(2 - d)\ell]$, whereas both g_2 and g_3 scale as $\exp[(2 + \mu - d)\ell]$ under these rescalings. Both the pure (g_1) and disorder (g_2 or g_3) nonlinearities naïvely scale the same way for short-ranged disorder ($\mu = 0$), making them compete with each other. Whether the resulting nonequilibrium steady state is controlled by g_1, or g_2 or g_3, or all of them, can only be ascertained by a RG treatment. In contrast, for spatially long-ranged disorders ($\mu > 0$), near a (stable) RG fixed point controlled by g_2 or g_3, g_1 is irrelevant in the RG sense. These can already be seen from the one-loop fluctuation corrections of the model parameters that with short-range quench disorder the corrections originating from the pure nonlinear term λ_1 have the same naïve infrared divergence as those originating from the disorder nonlinear term κ_1. Thus, both types of the fluctuation-corrections must be retained for a RG treatment. In contrast, for long-ranged disorder, the former class is necessarily less infrared divergent than the latter class [see Appendix C, Eqs. (C1)]. Therefore, in this case only the latter class of fluctuation-corrections is to be retained, and the former class discarded being less divergent, in the spirit of the RG procedure.

Note that at 1D the strength $D_T = 0$, it implies $g_2 = 0$ and $\gamma = 0$. The relevant one-loop Feynman diagrams are shown in Appendix C 1. The differential RG recursion relations for the model parameters are

$$\frac{dD_1}{d\ell} = D_1\left[z - d - 2\chi_h + \frac{g_1}{4} + 2g_3\right], \tag{15a}$$

$$\frac{d\nu_1}{d\ell} = \nu_1\left[z - 2 + \frac{2-d}{4d}g_1 + 2g_3\left(\gamma\frac{d-1}{d} + \frac{\mu-d}{2d}\right)\right], \tag{15b}$$

$$\frac{d\lambda_1}{d\ell} = \lambda_1\left[z + \chi_h - 2 + 2g_3\left(\gamma\frac{d-1}{d} - \frac{1}{d}\right)\right], \tag{15c}$$

$$\frac{d\kappa_1}{d\ell} = \kappa_1\left[z - 1 + \frac{\mu-d}{2} - \frac{2}{d}g_3\right], \tag{15d}$$

along with $dD_L/dl = 0 = dD_T/dl$. The flow Eqs. (15) can be used to find the RG flow of the dimensionless couplings g_1 and g_3. We get

$$\frac{dg_1}{d\ell} = g_1\left\{2 - d + \frac{g_1}{4}\left(4 - \frac{6}{d}\right) - g_3\left[2\gamma\left(1 - \frac{1}{d}\right) + \left(\frac{3\mu+4}{d} - 5\right)\right]\right\}, \tag{16a}$$

$$\frac{dg_3}{d\ell} = g_3\left\{2 + \mu - d - \frac{g_1}{2}\left(\frac{2}{d} - 1\right) - g_3\left[4\gamma\left(1 - \frac{1}{d}\right) + 2\left(\frac{\mu+2}{d} - 1\right)\right]\right\}. \tag{16b}$$

Below we discuss the scaling behavior for short-range and long-range correlated disorders separately using the flow Eqs. (16a) and (16b).

1. Short-range disorder

For the short-range disorder case, we set $\mu = 0$ as discussed earlier. The RG flow equations of g_1 and g_3 are

$$\frac{dg_1}{dl} = g_1\left\{2 - d + \frac{g_1}{4}\left(4 - \frac{6}{d}\right)\right.$$
$$\left. - g_3\left[2\gamma\left(1 - \frac{1}{d}\right) - \left(5 - \frac{4}{d}\right)\right]\right\}, \tag{17a}$$

$$\frac{dg_3}{dl} = g_3\left\{2 - d + \frac{g_1}{2}\left(1 - \frac{2}{d}\right)\right.$$
$$\left. - g_3\left[4\gamma\left(1 - \frac{1}{d}\right) + 2\left(\frac{2}{d} - 1\right)\right]\right\}. \tag{17b}$$

Flow Eqs. (17a) and (17b) show that both g_1 and g_3 have the same critical dimension 2. The flow equations in Eq. (17) at 2D have the form

$$\frac{dg_1}{dl} = g_1\left[\frac{g_1}{4} - g_3(\gamma - 3)\right], \quad \frac{dg_3}{dl} = -2\gamma g_3^2. \tag{18}$$

In Eqs. (18) (0,0) is the only fixed point. Further, g_3 flows to zero in the long RG time limit. In fact, the fixed point (0,0) is *stable* along the g_3 direction, whereas *unstable* along the g_1 direction. We further find that for any "initial conditions" $g_1(\ell = 0) > 0$, $g_3(\ell = 0) > 0$, the flow ultimately runs away along the g_1 axis to infinity suggesting the existence of a perturbatively inaccessible phase. Since g_3 flows to zero, we are tempted to speculate that this inaccessible phase is statistically identical to perturbatively inaccessible rough phase of the 2D KPZ equation.

The Gaussian fixed point (0,0) is unstable for dimension at or below $d = 2$ and it is the only FP at 2D. For any dimension higher than $d = 2$, the Gaussian fixed point is stable and the nonlinear terms are irrelevant near it. As a result, the scaling

properties are described by linear theory. For $d > 2$, there is at least one strong coupling fixed point corresponding to a rough phase, which is perturbatively inaccessible. While this is qualitatively similar to the pure KPZ equation, due to the nonperturbative nature of the rough phase, we cannot tell whether this rough phase is statistically same as the rough phase of $d > 2$ pure KPZ equation implying irrelevance of the quenched disorder, or different, in which case, quenched disorder is relevant. In the latter case, we speculate the yet unknown scaling properties are to be parametrized by the parameter γ. Numerical solutions of Eq. (12), or simulations of suitably constructed discrete models equivalent to Eq. (12) should be able to shed further light on this issue. Unsurprisingly, we further conclude that $d = 2$ is the lower critical dimension of Eq. (12), same as for the pure KPZ model.

We now briefly consider the scaling properties at $d = 1$ by performing the RG at $d = 1$, instead of expanding about the critical dimension [19,20]. Remembering $\gamma = 0$, the flow equations of g_1 and g_3 are

$$\frac{dg_1}{dl} = g_1\left[1 - \frac{g_1}{2} + g_3\right], \tag{19a}$$

$$\frac{dg_3}{dl} = g_3\left[1 - \frac{g_1}{2} - 2g_3\right]. \tag{19b}$$

The Fixed points are found by setting $\frac{dg_1}{dl} = 0 = \frac{dg_3}{dl}$ and corresponding stability are given below.

(1) (0,0): globally unstable.

(2) $(0, \frac{1}{2})$: stable in the g_3 direction and unstable in the g_1 direction.

(3) (2,0): stable in the g_1 direction, and marginally stable in the g_3 direction. At this stable fixed point, from Eqs. (15a) and (15b) we get the scaling exponents $z = 3/2$ and $\chi_h = 1/2$, which characterizes the KPZ universality class behavior.

The RG flow diagram is pictorially shown in Fig. 1.

We thus conclude that the short-range orientational quenched disorder is irrelevant in Eq. (12), ultimately giving the well-known 1D KPZ universality class.
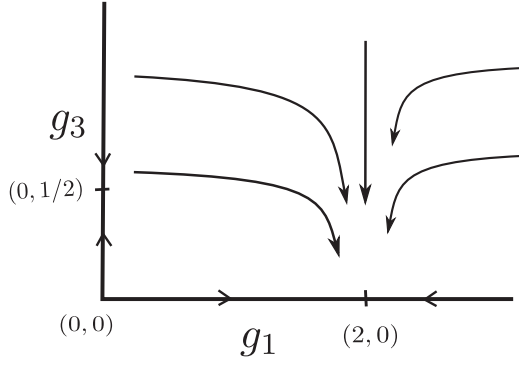
FIG. 1. Schematic flow diagram in the g_1-g_3 plane for the disordered KPZ equation at 1D, showing the irrelevance of the short-ranged quenched disorder (see text). Here, (2,0) is the stable fixed point.

2. Long-range correlated disorder

In this Section, we study the effects of spatially correlated or long-range disorder (i.e., $0 < \alpha < d$, i.e., $\mu > 0$) on the universal scaling properties of the KPZ equation. The flow Eqs. (16a) and (16b) show the critical dimension of $g_1 = 2$ but for g_2 is $2 + \mu$. Thus, coupling g_1 has a critical dimension lower than g_3. Therefore, g_1 is subleading to g_3, and the leading scaling behavior in the asymptotic long wavelength limit should be controlled by g_3 (if the disorder is relevant in the RG sense). Since g_1 is subleading, the renormalized disordered equation motion is invariant under inversion of h, a symmetry absent microscopically and also in the rough phase of the pure KPZ equation. Thus, this symmetry under inversion of h appears as an *emergent symmetry* of the model in the asymptotic long wavelength limit. The flow Eq. (16b) for g_3 is

$$\frac{dg_3}{dl} = g_3 \left\{ 2 + \mu - d - g_3 \left[4\gamma \left(1 - \frac{1}{d} \right) + 2 \left(\frac{\mu + 2}{d} - 1 \right) \right] \right\}.$$ (20)

To calculate the scaling exponents at dimensions $d < 2 + \mu$, we use $\mathcal{O}(\epsilon_1)$ expansion, where $d = 2 + \mu - \epsilon_1$, $\epsilon_1 > 0$. To the lowest order in $\mathcal{O}(\epsilon_1)$, the flow Eq. (20) for g_3 takes the form:

$$\frac{dg_3}{d\ell} = g_3 \left[\epsilon_1 - \frac{1 + \mu}{2 + \mu} 4\gamma g_3 \right].$$ (21)

Equation (21) reveals that $g_3^* = 0$ is an unstable fixed point, but

$$g_3^* = \frac{\epsilon_1}{4\gamma} \frac{2 + \mu}{1 + \mu}$$ (22)

for a nonzero γ is a stable fixed point. We evaluate the exponents at this stable fixed point. We find the dynamic exponent

$$z = 2 - \frac{\epsilon_1}{2\gamma} \frac{\gamma(1 + \mu) - 1}{(1 + \mu)},$$ (23)

which can be more or less than 2, its value in the linear theory, implying that nonlinear disorder effects can induce slower

or faster than ordinary diffusive relaxation of fluctuations, with $\gamma(1 + \mu) = 1$ is the boundary between the two kinds of behavior. We further get the roughness exponent

$$\chi_h = \frac{\epsilon_1}{4} \left[1 + \frac{3 + \mu}{\gamma(1 + \mu)} \right] - \frac{\mu}{2}.$$ (24)

Thus, both z and χ_h explicitly vary with γ. In the limit of $\gamma \to \infty$, i.e., for $D_T \gg D_L$, $z = 2 - \epsilon_1/2$ and $\chi_h = \epsilon_1/4 - \mu/2$. We focus on the $d = 2$ case. From the definition of ϵ_1, $d = 2$ implies $\epsilon_1 = \mu$. From Eq. (57), we then obtain

$$\chi_h = \frac{\mu}{4} \left[-1 + \frac{3 + \mu}{\gamma(1 + \mu)} \right],$$ (25)

which can be positive or negative, depending upon γ. In fact, for a large γ, $\chi_h < 0$. By setting $\chi_h = 0$, we get γ_c, the critical value of γ:

$$\gamma_c = (3 + \mu)/(1 + \mu).$$ (26)

Now, $\chi_h < 0$, which for a fluctuating surface means a "smooth surface", means $\langle h^2(\mathbf{x}, t) \rangle$ is independent of the system size L for large L. This, when h is interpreted as a phase, implies *long-range orientational order* in 2D, result not possible in equilibrium at 2D due to the well-known Mermin-Wagner theorem (MWT) [32]. Similarly, for an active membrane, this result means the membrane should be statistically flat, an impossibility in equilibrium again due to MWT. Since in 2D, $\epsilon_1 = \mu$ and $\mu = d - \alpha$, the maximum value of ϵ_1 can be 2 ($= \mu$ at 2D), by using this value we find $\chi_h = \frac{1}{2}[-1 + \frac{5}{3\gamma}]$, which can be made negative for $\gamma > 5/3$.

For $\epsilon_1 < 0$, i.e., $d > 2 + \mu$, $g_3 = 0$ is the only fixed point which is stable. We therefore conclude that $d = 2 + \mu$ is the *upper critical dimension* of this model.

At $d = 1$, in which case $D_T = 0$ necessarily, giving $\gamma = 0$. Then Eq. (21) reads

$$\frac{dg_3}{d\ell} = g_3 \epsilon_1.$$ (27)

For 1D, we set $\epsilon_1 = 1 + \mu$. The only fixed point here is $g_3^* = 0$, which is unstable. The lack of a stable fixed point does not allow us to extract the scaling properties. It is likely to be an artifact of the one-loop study. Notice that at any d-dimension for $\gamma \to 0$, *both* z and χ_h diverge in Eqs. (23) and (24), respectively, which is unphysical. To investigate the $\gamma = 0$ case further, we use Eq. (20) and perform a fixed dimension RG, which is similar in spirit with the RG for the 1D KPZ equation [20]; see also Refs. [19,33]. In that scheme Eq. (20) gives at d-dimension the stable fixed point

$$g_3^* = \frac{d}{2} \cdot \frac{2 + \mu - d}{2\gamma(d - 1) + 2 + \mu - d}.$$ (28)

At this fixed point, the scaling exponents can be calculated from Eqs. (15a) and (15b). We obtain

$$z = 2 - \frac{(2 + \mu - d)[2\gamma(d - 1) + \mu - d]}{2[2\gamma(d - 1) + 2 + \mu - d]},$$

$$\chi_h = \frac{2 - d}{2} - \frac{(2 + \mu - d)[2\gamma(d - 1) + \mu + d]}{4[2\gamma(d - 1) + 2 + \mu - d]}.$$ (29)

Thus, for $\gamma = 0$,

$$z = 2 - \frac{\mu - d}{2}, \tag{30}$$

$$\chi_h = \frac{2 - d}{2} - \frac{\mu + d}{4}, \tag{31}$$

which are perfectly well-behaved. In particular, at 1D, we find $g_3^* = 1/2$, $z = 2 - \frac{\mu - 1}{2}$ and $\chi_h = 1 - \frac{\mu + 1}{4}$. Further, using Eq. (29) we find in 2D $\chi_h = -\frac{\mu(2\gamma + 2 + \mu)}{4(2\gamma + \mu)}$ which gives a smooth surface whatever value of μ and γ. Generally then, regardless of the scheme we used, we uncover explicit γ-dependence of z and χ_h. This clearly shows parametrization of the universality classes by γ.

In general, an alert reader will easily notice that the roughness exponent in Eq. (24) from ϵ_1 expansion RG, or in Eq. (29) from fixed dimension RG method reveals that by tuning μ, it can be made positive or negative for $d < 2 + \mu$. Thus, by changing μ, the surface can be made rough ($\chi_h > 0$) or smooth ($\chi_h < 0$). The transition line in the $\mu - d$ plane can be found by setting $\chi_h = 0$. By using Eq. (24), we find the equation for the line

$$d = 2 + \mu - \frac{2\mu\gamma(1 + \mu)}{\gamma(1 + \mu) + 3 + \mu}, \tag{32}$$

in the ϵ_1-expansion calculation, and by using Eq. (29), the line is given by

$$2 - d = \frac{(2 + \mu - d)[2\gamma(d - 1) + \mu + d]}{2[2\gamma(d - 1) + 2 + \mu - d]}, \tag{33}$$

in the fixed dimension RG calculation. On the line $\chi_h = 0$, the surface is *logarithmically rough*. The dynamic exponent z on that line unsurprisingly depends on the precise equation of the line $\chi_h = 0$. We show for two differenty method: $z = 2 + \frac{\mu[1 - \gamma(1 + \mu)]}{3 + \mu + \gamma(1 + \mu)}$ by using Eq. (32) in ϵ_1 expansion case and $z = d + \frac{d(2 + \mu - d)}{2\gamma(d - 1) + 2 + \mu - d}$ by using Eq. (33) in fixed dimension RG analysis.

We plot the values of the scaling exponents as obtained from fixed dimension RG and ϵ_1 expansion as functions of γ in Fig. 2 below.

It is theoretically interesting to calculate the scaling exponents at the critical dimension $d = 2 + \mu$. The flow equation of g_3 is at $d = 2 + \mu$ reads [see Eq. (21)]

$$\frac{dg_3}{d\ell} = -\frac{1 + \mu}{2 + \mu} 4\gamma g_3^2. \tag{34}$$

Equation (34) shows that $g_3(\ell)$ is marginally irrelevant; $g_3(\ell)$ flows toward $g_3^* = 0$ with increasing of ℓ. Coupling $g_3(\ell)$ takes the form $g_3(\ell) = \frac{g_3(0)}{1 + g_3(0)\ell 4\gamma(\frac{1 + \mu}{2 + \mu})}$, and for large renormalization group time i.e., $\ell \to \infty$, $g_3(\ell) \simeq \frac{2 + \mu}{4\gamma(1 + \mu)} \frac{1}{\ell}$. This shows that timescale t no longer shows simple scale with length-scale r, giving breakdown of conventional dynamic scaling

$$t \sim r^2 [\log(r/a_0)]^{-\frac{\gamma(1 + \mu) - 1}{2\gamma(2 + \mu)}}. \tag{35}$$

Thus, the extent of breakdown of dynamic scaling depends on γ, and it can be faster or slower than ordinary diffusion. We now calculate the variance of h at the critical dimension
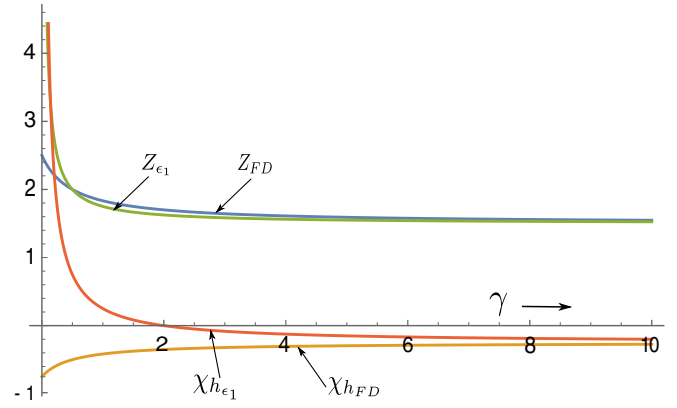

FIG. 2. A plot of the scaling exponents of the quenched disordered KPZ equation, comparing between the results found from one-loop ϵ_1 expansion and fixed dimension RG, showing the γ-dependence of the scaling exponents. Here, suffix ϵ_1 indicates scaling exponents obtained from an ϵ_2-expansion, whereas suffix FD indicates fixed dimension RG results. These are plotted for $d = 2$ and $\mu = 1$.

$d = 2 + \mu$. We get

$$\langle h^2(\mathbf{x}, t) \rangle \simeq \int_{1/L}^{1/a_0} d^{2 + \mu}\mathbf{q}\, q^{-2}[\log(1/q)]^{-\frac{\gamma(1 + \mu) - (3 + \mu)}{2\gamma(2 + \mu)}}. \tag{36}$$

Here, L and a_0 are linear system size and small-scale cutoff, respectively. Clearly, $\langle h^2(\mathbf{x}, t) \rangle$ is bounded: it does not diverge for large L. For $d > 2 + \mu$, i.e., above the upper critical dimension, since $g_3 = 0$ is the stable FP, the asymptotic long wavelength limit scaling is identical to the linear theory.

We thus find that with short-range disorder although the disorder coupling constant g_3 is naïvely as relevant as the coupling g_1 of the pure KPZ equation, in a one-loop theory g_3 is irrelevant in the RG sense at all dimensions. For long-range correlated disorder g_3 is relevant while g_1 becomes irrelevant, resulting into scaling exponents depending explicitly on γ. Last, for $\mu < 0$ quenched disorder is irrelevant in all dimensions. Hence, the model belongs to the standard KPZ universality class. In fact, this model with $\mu < 0$ is statistically identical to $\mu = 0$ in the long wavelength limit.

We present the phase diagram of the disordered KPZ equation in the $\mu - d$ plane showing the possible phases in Fig. 3.

B. Quenched disordered CKPZ equation

We now investigate the universal scaling properties of the quenched disordered CKPZ equation. As in our study of the disordered KPZ equation above, we consider both short-ranged and long-ranged disorders separately. In the linear limit of Eq. (14), we find dynamic exponent $z = 4$ and roughness exponent $\chi_h = \frac{2 - d}{2}$, which are unsurprisingly identical to the scaling of the linearlized pure CKPZ equation; see Appendix B 2 for detailed calculations. The nonlinear terms can affect the linear theory theory scaling, if they are relevant in a RG sense. For instance, the pure CKPZ equation has an upper critical dimension two, meaning for dimension $d < 2$, the nonlinear effects modify the linear theory scaling in the asymptotic long wavelength limit. In the disordered case,
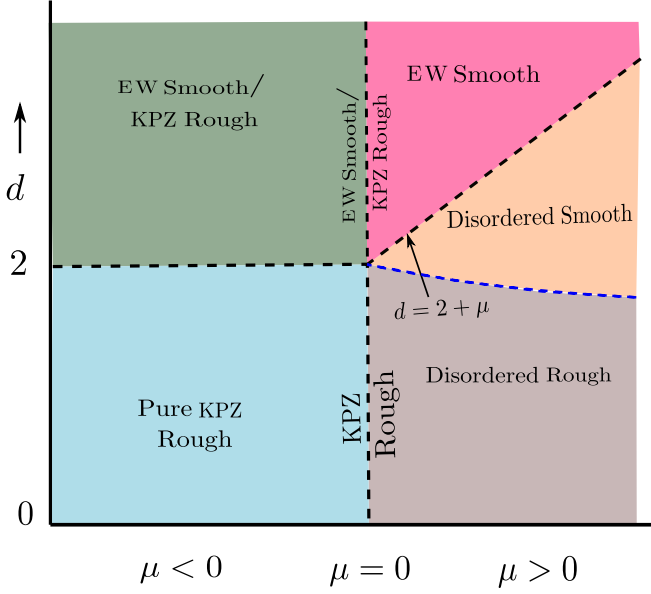
FIG. 3. Schematic phase diagram of the quenched disordered KPZ equation in the μ-d plane. The broken blue line corresponds to $\chi_h = 0$, dividing the disorder-induced rough and smooth phases, and depends on γ; here, this line is schematically drawn for $\gamma = 1$.

as for the quenched disordered KPZ equation, the pertinent questions are, whether disorder is relevant in the RG sense, and if so, what are scaling properties of the resulting universality class. We systematically address these issues by using one-loop perturbative RG, whose details are available in the Appendix C.

Similar to our studies above on the quenched disordered KPZ equation, we define two dimensionless coupling constants $\Theta_1 = \frac{\lambda_2^2 D_2}{\nu_2^3}\tilde{K}_d$, $\Theta_2 = \frac{\kappa_2^2 D_T}{\nu_2^2}\tilde{K}_d$, and $\Theta_3 = \frac{\kappa_2^2 D_L}{\nu_2^2}\tilde{K}_d$. Further, we set D_L and D_T do not scale, accordingly we define a ratio $\gamma = \frac{D_T}{D_L} \equiv \frac{\Theta_2}{\Theta_3}$. Note that at 1D the strength $D_T = 0$, which implies $\gamma = 0$, as before. Furthermore, naïve rescaling of space, time and the fields, as shown in Appendix C 2 show

that the under these rescalings, effective couplings Θ_1 scales as $\exp[(2-d)\ell]$, whereas both Θ_2 and Θ_3 scale as $\exp[(2+\mu-d)\ell]$. As in the RG treatment of the disordered KPZ equation, in the RG analysis for the CKPZ equation, both the pure (Θ_1) and disorder (Θ_2 or Θ_3) nonlinearities naïvely scale the same way for short-ranged disorder, making them compete with each other and control the nonequilibrium steady states. In contrast, for spatially long-ranged disorders $\mu > 0$, Θ_2 or Θ_3 control the behavior of stedy states, Θ_1 is irrelevant in the RG sense. The one-loop fluctuation-corrections generating from pure λ_2 and disorder κ_2 nonlinearities show these two types of infrared divergences [see Appendix C, Eqs. (C2)]. With short-range disorder, both types have the same divergences, but for long-range disorder the leading divergences originate from the disorder vertices. Needless to say, as for the disordered KPZ equation studied above, in all these cases the parameter γ is marginal, and has no fluctuation-corrections. This means there is no need to study the flows of Θ_2 and Θ_3 separately; it is enough to study the flow of one of them parametrized by γ. In what follows below, we choose to work with Θ_1 and Θ_3.

The RG recursion relation of the model parameters for general $\mu \geqslant 0$ are (see Appendix C for more details):

$$\frac{dD_2}{d\ell} = D_2[z - d - 2 - 2\chi_h], \tag{37a}$$

$$\frac{d\nu_2}{d\ell} = \nu_2\left[z - 4 + \frac{4-d}{4d}\Theta_1 + 2\Theta_3\left(\gamma\frac{d-1}{d} + \frac{\mu-d}{2d}\right)\right], \tag{37b}$$

$$\frac{d\lambda_2}{d\ell} = \lambda_2\left[z + \chi_h - 4 + 2\Theta_3\left(\gamma\frac{d-1}{d} - \frac{1}{d}\right)\right], \tag{37c}$$

$$\frac{d\kappa_2}{d\ell} = \kappa_2\left[z - 3 + \frac{\mu-d}{2} - \frac{2}{d}\Theta_3\right]. \tag{37d}$$

The flow equations of the dimensionless coupling constants Θ_1 and Θ_3 are then calculated by using Eqs. (37). These are given by

$$\frac{d\Theta_1}{d\ell} = \Theta_1\left[2 - d - \frac{4-d}{4d}3\Theta_1 - \Theta_3\left(2\gamma\frac{d-1}{d} + \frac{4+3\mu-3d}{d}\right)\right], \tag{38a}$$

$$\frac{d\Theta_3}{d\ell} = \Theta_3\left\{2 + \mu - d - \frac{4-d}{2d}\Theta_1 - \Theta_3\left[\frac{d-1}{d}4\gamma + 2\left(\frac{2+\mu-d}{d}\right)\right]\right\}. \tag{38b}$$

We separately discuss the short and long-range disorder cases below.

1. Short-range disorder

When the disorder is short-ranged, we set $\mu = 0$. The flow equations of couplings Θ_1 and Θ_3 for the short-ranged disorder case can be obtained from Eq. (37). These are

$$\frac{d\Theta_1}{d\ell} = \Theta_1\left[2 - d - \frac{4-d}{4d}3\Theta_1 - \Theta_3\left(2\gamma\frac{d-1}{d} + \frac{4-3d}{d}\right)\right], \tag{39a}$$

$$\frac{d\Theta_3}{d\ell} = \Theta_3\left[2 - d - \frac{4-d}{4d}2\Theta_1 - 2\Theta_3\left(2\gamma\frac{d-1}{d} + \frac{2-d}{d}\right)\right]. \tag{39b}$$
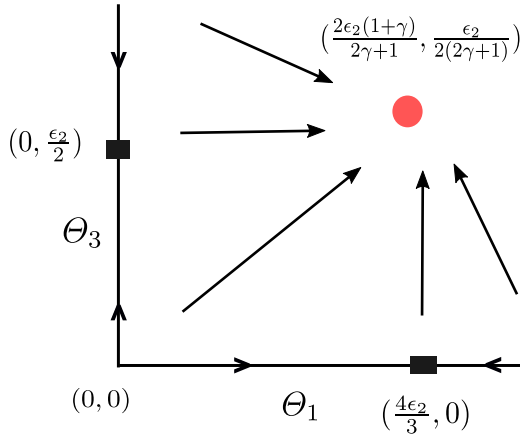
FIG. 4. Schematic flow diagram at dimension $d = 2 - \epsilon_2$, $\epsilon_2 > 0$ (except 1D) for the short-range quenched disordered CKPZ equation. The small, red circle is the nontrivial fixed point, which is globally stable.

Flow Eqs. (39a) and (39b) show that Θ_1 and Θ_3 both have the same critical dimension 2, as already argued by using naïve rescaling of space, time and the fields. Further, the Gaussian fixed point (0,0) is globally unstable below 2D, whereas this is the only stable fixed point at or above 2D. That implies that $d = 2$ is the upper critical dimension for this model, same as pure CKPZ; at 2D, couplings Θ_1 and Θ_3 are *marginally irrelevant*. Therefore, the linear theory scaling is expected to be modified by the nonlinear effects at or below 2D, whereas for $d > 2$ the nonlinear couplings are irrelevant and the linear theory holds in the asymptotic long wavelength limit. To the lowest order in $\epsilon_2 \equiv 2 - d$, the flow Eqs. (39a) and (39b) reduce to

$$\frac{d\Theta_1}{d\ell} = \Theta_1 \left[\epsilon_2 - \frac{3\Theta_1}{4} - \Theta_3(\gamma - 1) \right], \quad (40a)$$

$$\frac{d\Theta_3}{d\ell} = \Theta_3 \left[\epsilon_2 - \frac{\Theta_1}{2} - 2\gamma\Theta_3 \right]. \quad (40b)$$

Equations (40a) and (40b) can be used to calculate the fixed points (Θ_1^*, Θ_2^*) by setting $\frac{d\Theta_1}{d\ell} = 0 = \frac{d\Theta_3}{d\ell}$. We find

(1) Fixed point 1: (0,0) is globally unstable.

(2) Fixed point 2: $(0, \epsilon_2/2)$ unstable in the Θ_1 direction, but stable in the Θ_3 direction.

(3) Fixed point 3: $(4\epsilon_2/3, 0)$ unstable in the Θ_3 direction, but stable in the Θ_1 direction.

(4) Fixed point 4: The nontrivial fixed point $(\frac{2\epsilon_2(1+\gamma)}{2\gamma+1}, \frac{\epsilon_2}{2(2\gamma+1)})$: stable along both the Θ_1 and Θ_2 directions, i.e., globally stable.

The fixed points and the RG flow lines are shown schematically in Fig. 4.

The globally stable fixed point describes the stable nonequilibrium steady state of the model. It can be used to calculate the associated scaling exponents. We find that the dynamic exponent

$$z = 4 - \frac{\epsilon_2 \gamma}{2\gamma + 1}, \quad (41)$$

and the roughness exponent

$$\chi_h = \frac{\epsilon_2(1 + \gamma)}{2(2\gamma + 1)}. \quad (42)$$

From this above expression $\chi_h > 0$ since $\epsilon_2 > 0$. Thus, it is a short-range disorder induced rough phase ("SR rough"). We note that as $\gamma \to 0$, both z and χ_h approach their linear theory values, i.e., $z = 4$, $\chi_h = \epsilon_2/2$, an unexpected result. In the same way, we note that at 1D, $\epsilon_2 = 1$ and $\gamma = 0$, giving $z = 4$, $\chi_h = \frac{1}{2}$, identical to the linear theory results! In the absence of any general symmetry argument to render the fluctuation corrections to vanish or turn irrelevant, we believe this is fortuitous, an artifact of the one-loop perturbation theory. Higher order perturbation theory or numerical studies should be useful to obtain better quantitative estimates of the exponents in the limit $\gamma \to 0$. We reanalyze the 1D case by using a fixed dimension RG scheme, which is similar in spirit with what one does for the 1D KPZ equation [20]. To do this, we use the flow Eqs. (39a) and (39b) directly, and set $d = 1$.

The resulting flow equations are

$$\frac{d\Theta_1}{d\ell} = [1 - 9\Theta_1/4 - \Theta_3], \quad (43)$$

$$\frac{d\Theta_3}{d\ell} = [1 - 3\Theta_1/2 - 2\Theta_3]. \quad (44)$$

Solving these two equations, (1/3, 1/4) is only stable FP and finds the exponents $z = 4$, $\chi_h = 1/2$, again same as the linear theory results, offering no further insight into the unexpected appearance of the linear theory results.

The fixed point analysis of the flow equations in 2D, which is the physically relevant dimension as its pure counterpart is, needs to be done separately, as 2D is the critical dimension. At $d = 2$, i.e., $\epsilon_2 = 0$. The resulting flow equations of Θ_1 and Θ_3 are

$$\frac{d\Theta_1}{d\ell} = -\Theta_1 \left[\frac{3\Theta_1}{4} + \Theta_3(\gamma - 1) \right], \quad (45a)$$

$$\frac{d\Theta_3}{d\ell} = -\Theta_3 \left[\frac{\Theta_1}{2} + 2\gamma\Theta_3 \right]. \quad (45b)$$

Thus, (0,0) is the *only* fixed point. Whether it is a stable or unstable fixed point can be found only by solving the flow Eqs. (45a) and (45b). To do so, we first define a ratio $\beta = \frac{\Theta_3}{\Theta_1}$. The flow equation of β is

$$\frac{d\beta}{d\ell} = \beta \Theta_1 \left[\frac{1}{4} - \beta(1 + \gamma) \right]. \quad (46)$$

Equation (46) shows that

$$\beta^* = \frac{1}{4(1 + \gamma)} = \frac{\Theta_3(\ell)}{\Theta_1(\ell)} \quad (47)$$

gives the fixed point of Eq. (46), which in turn gives the *separatrix*, such that all initial conditions $\Theta_1(\ell=0)$, $\Theta_3(\ell=0)$ maintaining $\Theta_3(\ell = 0)/\Theta_1(\ell = 0) = \beta^*$ will continue to maintain it under the RG transformations. Furthermore, the separatrix can be shown to be *stable* or *attractive*: We write $\beta = \beta^* + \delta\beta$. To the linear order in $\delta\beta$, we find

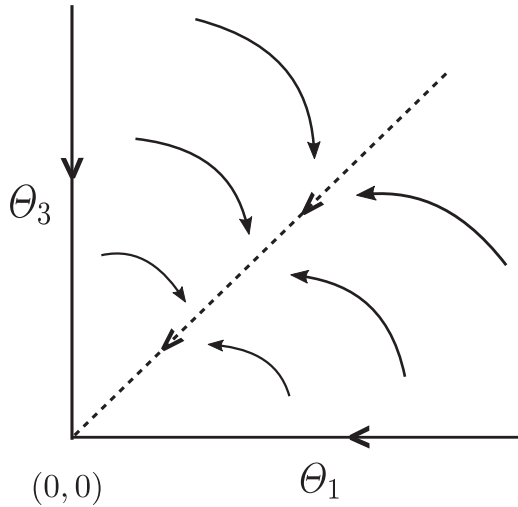$$\frac{d\delta\beta}{\delta\ell} = -\beta^* \Theta_1(1 + \gamma)\delta\beta, \quad (48)$$

FIG. 5. Schematic RG flow diagram in 2D ($\epsilon_2 = 0$) for the short-range quenched disordered CKPZ equation. The origin (0,0) is the only fixed point, which is stable. The incline straight line is the separatrix having a γ-dependent slope given by Eq. (47).

showing the attractive nature of the separatrix. Interestingly, as $\gamma \to \infty$, $\beta^* \to 0$, meaning that the separatrix coincides with the Θ_1 axis in the Θ_1-Θ_3 plane in that limit. Using the value of β^*, we can further show that

$$\frac{d\Theta_1(\ell)}{d\ell} = -\frac{\Theta_1^2(1+2\gamma)}{2(1+\gamma)} < 0, \qquad (49a)$$

$$\frac{d\Theta_3(\ell)}{d\ell} = -\Theta_3^2 2(1+2\gamma) < 0, \qquad (49b)$$

giving (0,0) as the *globally stable* fixed point. This then means Θ_1 and Θ_3 are *marginally irrelevant*, with both of them eventually flowing to zero in the asymptotic long wavelength limit. Nonetheless, they do so slowly enough to allow for infinite renormalization of ν_2, leading to logarithmic modulations of the linear theory scaling. We work this out explicitly below.

Since the separatrix is attractive, we can use $\Theta_3(l) = \beta^*\Theta_1(l)$ in the long wavelength limit in the flow Eq. (45a). We can then solve the resulting effective flow equation for $\Theta_1(l)$ giving

$$\Theta_{1l} = \frac{2(1+\gamma)}{1+2\gamma}\frac{1}{\ell}, \quad \Theta_{3l} = \frac{1}{2(1+2\gamma)}\frac{1}{\ell}, \qquad (50)$$

is the asymptotic limit $\ell \to \infty$. Since ℓ is the logarithm of a physical length scale, we note that both $\Theta_1(\ell)$ and $\Theta_3(\ell)$ approach zero logarithmically slowly. Thus, an arbitrary initial condition $\Theta_1(\ell = 0)$, $\Theta_3(\ell = 0)$ not only *flows to* the origin, it also *flows toward* the attractive separatrix in course of its flow to the origin under successive RG transformations. The RG flows in 2D are schematically shown in Fig. 5.

We can now find the scale-dependent $\nu_2(\ell)$ by assuming $z = 4$, $\chi_h = 0$. This gives

$$\nu_2(\ell) \simeq \nu_2(0)\ell^{\frac{\gamma}{2\gamma+1}}. \qquad (51)$$

However, $D_2(\ell) \simeq D_2(0)$, since it has no relevant one-loop fluctuation correction.

These can be used to obtain the variance

$$\langle h^2(\mathbf{x}, t)\rangle \sim [\log(L/a_0)]^{1-\frac{\gamma}{1+2\gamma}}, \qquad (52)$$

where L and a_0 are linear system size and small-scale cutoff, respectively. The logarithmic dependence of $\langle h^2(\mathbf{x}, t)\rangle$ on the system size L in Eq. (52) implies that at $d = 2$, the disordered CKPZ surface is *logarithmically rough* ("log rough"). We further see that in the renormalized theory, timescale t and length-scale r are no longer simply related by a dynamic scaling exponent. We in fact find

$$t \sim r^4[\log(r/a_0)]^{-\frac{\gamma}{1+2\gamma}} \qquad (53)$$

for large r, signifying breakdown of conventional dynamic scaling due to logarithmic modulations. The dynamics is logarithmically slower than that in the linear theory by an extent that depends upon γ. In the limit $\gamma = 0$ ($D_T = 0$), $t \sim r^4$, same as in the linear theory, which is likely an artifact of our low order perturbation theory; as γ rises, the dynamics gets slower initially, ultimately saturating at $t \sim r^4 \frac{1}{\sqrt{\log(r/a_0)}}$ as $\gamma \to \infty$, i.e., $D_T \gg D_L$. In the same limit by using Eq. (52), we obtain $\langle h^2(\mathbf{x}, t)\rangle \sim \sqrt{\log(L/a_0)}$.

2. Long-range correlated disorder

We now study the scaling properties in the presence of long-range quenched disorder, i.e., $\alpha < d$, or $\mu > 0$. The flow Eqs. (38a) and (38b) show that the critical dimensions of $\Theta_1 = 2$ but for Θ_3 is $2 + \mu > 0$. Here Θ_1 has critical dimension lower than Θ_3. Therefore, near a fixed point controlled by Θ_3, Θ_1 is subleading to Θ_3, and the leading scaling behavior is described by Θ_3. This is similar to our analysis for the long-range quenched disordered KPZ equation above. Again, as in the disordered KPZ equation, the disordered CKPZ equation with long-range disorder has invariance under inversion of h as an emergent symmetry in the long wavelength limit. Hence, Eq. (38b) reduces to

$$\frac{d\Theta_3}{dl}$$
$$= \Theta_3\left\{2 + \mu - d - \Theta_3\left[4\gamma\left(1 - \frac{1}{d}\right) + 2\left(\frac{\mu+2}{d} - 1\right)\right]\right\}. \qquad (54)$$

Notice that Eq. (54) is identical to the flow Eq. (20) in Sec. IV A 2, and hence, the ensuing analysis runs exactly parallel to the one below Eq. (20) in Sec. IV A 2. To proceed further, we set $d = 2 + \mu - \epsilon_2$ where $\epsilon_2 > 0$ and extract the fixed point and the associated scaling exponents to $\mathcal{O}(\epsilon_2)$. The flow equation of Θ_3 reads

$$\frac{d\Theta_3}{d\ell} = \Theta_3\left[\epsilon_2 - \frac{1+\mu}{2+\mu}4\gamma\Theta_3\right]. \qquad (55)$$

Unsurprisingly, Eq. (55) is same as Eq. (21) in Sec. IV A 2. Equation (55) gives $\Theta_3 = 0$ is an unstable fixed point, but $\Theta_3 = \Theta_3^* \equiv \frac{\epsilon_2}{4\gamma}\frac{2+\mu}{1+\mu}$ is a stable *fixed point* for any $\gamma > 0$. As before, the scaling exponents are calculated at the stable fixed point Θ_3^*. We find the dynamic exponent

$$z = 4 - \frac{\epsilon_2}{2\gamma}\frac{\gamma(1+\mu) - 1}{1+\mu}, \qquad (56)$$
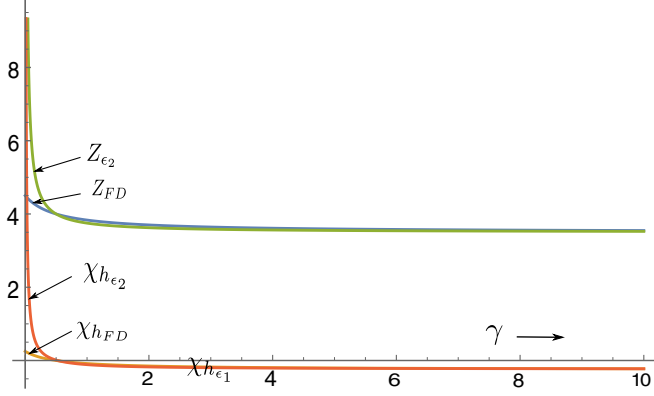
FIG. 6. The scaling exponents are plotted as functions of γ to compare between the results found from one-loop ϵ_2 expansion RG and fixed dimension RG. Here, suffix ϵ_2 indicates scaling exponents obtained from an ϵ_2-expansion, whereas suffix FD indicates fixed dimension RG results. We have set $d = 2$, $\mu = 1$.

which can be lesser or greater than 4, with the dynamics being faster or slower, respectively, than in the linear theory. Further, the roughness exponent

$$\chi_h = \frac{\epsilon_2}{4}\left[1 + \frac{1}{\gamma(1+\mu)}\right] - \frac{\mu}{2}. \quad (57)$$

Clearly, both z and χ depends explicitly on and vary continuously with γ. As $\gamma \to \infty$, $z = 4 - \epsilon_2/2$, $\chi_h = \epsilon_2/4 - \mu/2$. However, if $\gamma \to 0$, i.e., $D_T \ll D_L$, then both z and χ_h diverge, an unexpected result reminiscent of what we have found in the analogous analysis for the long-range disordered KPZ equation. At 1D, necessarily $\gamma = 0$, the flow of Θ_3 reads same as Eq. (27),

$$\frac{d\Theta_3}{d\ell} = \Theta_3 \epsilon_2. \quad (58)$$

Equation (58) surprisingly has no stable FP, so it cannot describe stable scaling behavior at 1D, which we believe just as an artifact of our one-loop calculations. To investigate this further, we perform a fixed dimension RG akin to the 1D KPZ equation [20]. In this scheme flow Eq. (54) has a fixed point $\Theta_3^* = \frac{d}{2} \cdot \frac{2+\mu-d}{2\gamma(d-1)+2+\mu-d}$ at a (fixed) dimension d, which is a stable fixed point. We calculate the exponents at this fixed point are

$$z = 4 - \frac{(2+\mu-d)[2\gamma(d-1)+\mu-d]}{2[2\gamma(d-1)+2+\mu-d]}, \quad (59a)$$

$$\chi_h = \frac{2-d}{2} - \frac{(2+\mu-d)[2\gamma(d-1)+\mu-d]}{4[2\gamma(d-1)+2+\mu-d]}. \quad (59b)$$

Thus, the scaling exponents depend explicitly on γ. These results reveal the generally expected existence of a stable scaling regime parametrized by γ different from the linear theory scaling.

We give a plot of the scaling exponents, showing their dependence on the disorder parameter γ in Fig. 6.

For $d = 1$ with $\gamma = 0$, the value of the fixed point is $\Theta_3 = 1/2$ and exponents are $z = 4 - \frac{\mu-1}{2}$ and $\chi_h = \frac{1}{2} - \frac{\mu-1}{4}$ using the values of Eqs. (59a) and (59b).

Similar to the disordered KPZ equation with long-range quenched disorder, both smooth and rough phases are possible for $d < 2 + \mu$, as can be seen from Eq. (57), obtained from an ϵ_1 expansion RG, and from Eq. (59b), obtained by using a fixed dimension RG method. As γ is varied, the system can undergo a transition between a smooth with $\chi_h < 0$ and a rough $\chi_h > 0$ phase. The transition line in the μ-d plane can be found from the condition $\chi_h = 0$, and is parametrized by γ. The equation of this line obtained from an ϵ_2 expansion RG is given by

$$d = 2 + \mu - \frac{2\mu\gamma(1+\mu)}{\gamma(1+\mu)+1}. \quad (60)$$

The same obtained from a fixed dimension RG scheme is given by

$$2 - d = \frac{(2+\mu-d)[2\gamma(d-1)+\mu-d]}{2[2\gamma(d-1)+2+\mu-d]}. \quad (61)$$

As expected and similar to the quenched disordered KPZ equation studied above, the location of these lines in the $\mu - d$ plane depend explicitly on γ. The surface is *logarithmically rough* on the line $\chi_h = 0$. The dynamic exponent z on this line will be $4 - \frac{\mu[\gamma(1+\mu)-1]}{\gamma(1+\mu)+1}$ by using Eq. (60) for ϵ_2 expansion case or $2 + d$ by using Eq. (61) for fixed dimension RG case.

We find that at 2D, $\epsilon_2 = \mu$ in the ϵ_2-expansion method, and hence from Eq. (57) $\chi_h = \frac{\mu}{4}[-1 + \frac{1}{\gamma(1+\mu)}]$. We further note that again in the fixed dimension RG method, by using $d = 2$, Eq. (59b) gives $\chi_h = -\frac{\mu(2\gamma+\mu-2)}{4(2\gamma+\mu)}$. On the whole, these show that χ_h can be negative depending on values of γ and μ. This means that the surface can be smooth due to presence of long-range disorder instead of logarithmically rough in pure CKPZ case.

Precisely at dimension $d = 2 + \mu$, the flow equation of g_2 is

$$\frac{d\Theta_3}{d\ell} = -\frac{1+\mu}{2+\mu}4\gamma\Theta_3^2. \quad (62)$$

Equation (62), which has the same structure as Eq. (34), reveals that $\Theta_3(\ell)$ is marginally irrelevant and it flows to zero with increasing of ℓ; in fact, $\Theta_3 = 0$ is the *only* fixed point, which is stable. Furthermore, $\Theta_3(\ell)$ scales as $\frac{2+\mu}{4\gamma(1+\mu)}\frac{1}{\ell}$ in the limit of large renormalization time length (ℓ), same as the behavior of $g_3(\ell)$ for large ℓ in Sec. IV A 2 above. This behavior of coupling constant realizes the leading scaling: dynamic exponent $z = 4$ and roughness exponent $\chi_h = -\mu/2$. This in turn gives breakdown of conventional dynamic scaling with

$$t \sim r^4[\log(r/a_0)]^{-\frac{\gamma(1+\mu)-1}{2\gamma(2+\mu)}}, \quad (63)$$

meaning the dynamics is logarithmically faster than the linear theory. Furthermore, the extent of "logarithmic speeding up" vis-a-vis the linear theory depends explicitly on γ, and also unsurprisingly on μ. The variance of h at $d = 2 + \mu$ is

$$\langle h^2(\mathbf{x}, t)\rangle \simeq \int_{1/L}^{1/a} \frac{d^{2+\mu}\mathbf{q}}{q^2}[\log(1/q)]^{-\frac{\gamma(1+\mu)-1}{2\gamma(2+\mu)}}. \quad (64)$$

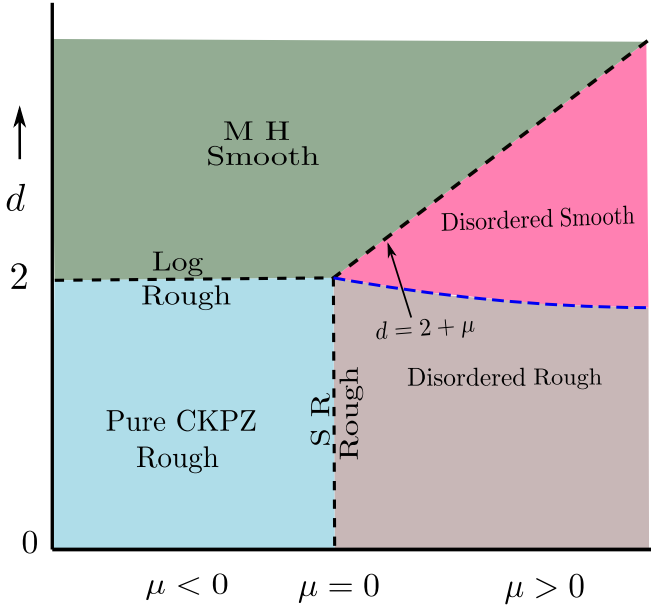The above expression says that variance does not diverge for large L.

FIG. 7. Schematic phase diagram of the disordered CKPZ equation in the μ-d plane. The broken blue line divides disorder induced rough and smooth phases and depends on disorder parameter γ; here this line is schematically drawn for $\gamma = 1$.

So far we have studied $\mu \geqslant 0$ above. In principle, one may also consider the case $\mu < 0$. This choice makes Θ_3 subdominant to Θ_1 at all dimensions, making the model identical to the pure CKPZ equation in the long wavelength limit. In fact, as in the case of quenched disorder KPZ equation above, the

$\mu < 0$ case for the CKPZ equation is statistically identical to the pure ckpz case in the long wavelength limit. Interestingly, the $\mu = 0$ case for the quenched disordered KPZ equation is statistically identical to the pure KPZ equation in the long wavelength limit; in contrast, the $\mu = 0$ case for the quenched disordered CKPZ equation belongs to a new universality class *different* from the pure CKPZ equation. This amply highlights the role of the conservation law in determining the universality classes in driven diffusive systems.

We summarize our results on the disordered CKPZ equation in the form of a phase diagram in Fig. 7 showing all the possible phases in μ-d plane.

We thus obtain the scaling exponents varying continuously with γ for both the short- and long-range disorder cases.

We summarize our results on the scaling exponents of the quenched disordered KPZ and CKPZ equations in the following Tables I and II, respectively.

V. SUMMARY AND OUTLOOK

In summary, we have studied the universal scaling properties of the KPZ and conserved KPZ equations coupled to orientational quenched disorders. We have chosen a particular form of disorder that couples with the local gradient of the height field, i.e., the disorder is sensitive to the local height nonuniformity. It is described by a zero-mean Gaussian distributed quenched vector field **V**. Vector **V** can in general have both irrotational and solenoidal parts. This is reflected in the variance of $\mathbf{V(k)}$ having parts proportional to the transverse $P_{ij}(\mathbf{k})$ and longitudinal projection operator $Q_{ij}(\mathbf{k})$, with amplitudes D_T and D_L, respectively. This allows us to define a dimensionless number $\gamma \equiv D_T / D_L$. We have

TABLE I. Scaling exponents for the disordered KPZ equation as obtained from both ϵ_1-expansion and fixed dimension RG.

	Disordered KPZ equation				
	$\mu = 0$: Uncorrelated disorder			$\mu > 0$: Correlated disorder	
Dim.	Exponents	Possible phases	Dim.	Exponents	Possible phases
$d < 2$	Pure KPZ result: Disorder irrelevant. At $d = 1$, $z = 3/2$ and $\chi_h = 1/2$.	Rough	$d < 2 + \mu$	ϵ_1 expansion: $z = 2 - \frac{\epsilon_1}{2\gamma}\frac{\gamma(1+\mu)-1}{(1+\mu)}$, $\chi_h = \frac{\epsilon_1}{4}[1 + \frac{3+\mu}{\gamma(1+\mu)}] - \frac{\mu}{2}$. Fixed dimension RG: $z = 2 - \frac{(2+\mu-d)[2\gamma(d-1)+\mu-d]}{2[2\gamma(d-1)+2+\mu-d]}$, $\chi_h = \frac{2-d}{2} - \frac{(2+\mu-d)[2\gamma(d-1)+\mu+d]}{4[2\gamma(d-1)+2+\mu-d]}$.	Disorder induced rough and smooth possible. At the transition $\chi_h = 0$ with $z = 2 + \frac{\mu[1-\gamma(1+\mu)]}{3+\mu+\gamma(1+\mu)}$ and $z = d + \frac{d(2+\mu-d)}{2\gamma(d-1)+2+\mu-d}$ for ϵ_1 expansion and fixed dimension RG case, respectively.
$d = 2 = d_{lc}$	Pure KPZ result.	Rough	$d = 2 + \mu = d_{uc}$	$z = 2$, $\chi_h = -\mu/2$.	Smooth
$d > 2$	EW result: $z = 2$, $\chi_h = \frac{2-d}{2}$, or the scaling exponents of the pertubatively inaccessible rough.	Smooth and rough with a roughening transition	$d > 2 + \mu$	EW result: $z = 2$, $\chi_h = \frac{2-d}{2}$.	Smooth

TABLE II. Scaling exponents for the disordered CKPZ equation as obtained from both ϵ_2-expansion and fixed dimension RG.

Disordered CKPZ equation					
$\mu = 0$: Uncorrelated disorder			$\mu > 0$: Correlated disorder		
Dim.	Exponents	Possible phases	Dim.	Exponents	Possible phases
$d = 1 < d_{uc} = 2$	ϵ_2 expansion with $\epsilon_2 = 1$: $z = 4 - \frac{\epsilon_2 \gamma}{2\gamma+1}$, $\chi_h = \frac{\epsilon_2(1+\gamma)}{2(2\gamma+1)}$. Fixed dimension RG: $z = 4$, $\chi_h = 1/2$.	Rough	$d < 2 + \mu$	ϵ_2 expansion: $z = 4 - \frac{\epsilon_2}{2\gamma}\frac{\gamma(1+\mu)-1}{1+\mu}$, $\chi_h = \frac{\epsilon_2}{4}[1 + \frac{1}{\gamma(1+\mu)}] - \frac{\mu}{2}$. Fixed dimension RG: $z = 4 - \frac{(2+\mu-d)[2\gamma(d-1)+\mu-d]}{2[2\gamma(d-1)+2+\mu-d]}$, $\chi_h = \frac{2-d}{2} - \frac{(2+\mu-d)[2\gamma(d-1)+\mu-d]}{4[2\gamma(d-1)+2+\mu-d]}$.	Disorder induced rough and smooth possible. At the transition $\chi_h = 0$ with $z = 4 - \frac{\mu[\gamma(1+\mu)-1]}{\gamma(1+\mu)+1}$ for ϵ_2 expansion case and $z = 2 + d$ for fixed dimension RG case.
$d = 2 = d_{uc}$	$z = 4$ and $\chi_h = 0$ with logarithmic roughness	Logarithmic rough or smooth	$d = 2 + \mu = d_{uc}$	$z = 4$, $\chi_h = -\mu/2$	Smooth
$d > 2$	MH result: $z = 4$, $\chi_h = \frac{2-d}{2}$.	Smooth	$d > 2 + \mu$	MH result: $z = 4$, $\chi_h = \frac{2-d}{2}$.	Smooth

studied the scaling properties of the models for both spatially short and long-ranged quenched disorders by using a one-loop perturbative RG scheme.

For each of the models, we have calculated the relevant scaling exponents, i.e., the roughness exponent χ_h and dynamic exponent z. For instance, we find that the disordered KPZ equations with short-ranged quenched disorder belongs to the well-known KPZ equation only, i.e., the disorder is irrelevant in the RG sense. Unsurprisingly, $d = 2$ remains the lower critical dimension of the model, just as it is for the pure KPZ equation. For long-range disorder, the model no longer belongs to the KPZ universality class; a new universality class emerges, with the pure KPZ nonlinear term being irrelevant in the RG sense. Our result on long-range orientational order induced by long-range quenched disorder, when h is considered as a phase, is theoretically intriguing, and should stimulate further work on disordered active *XY* models. The asymptotic long wavelength scaling is controlled by the disorder nonlinearity only, and the associated scaling exponents depend explicitly on γ and μ; the latter parameter characterizes the spatial scaling of the disorder variance. In contrast, for the disordered CKPZ equation, even with short-range disorder we find that a new universality class emerges at dimension $d \leqslant 2$; the scaling exponents are calculated by using a one-loop expansion, which depend explicitly on γ. Further, $d = 2$ is now the upper critical dimension, as in the pure CKPZ equation. For long-range disorder, the pure CKPZ nonlinearity is irrelevant in the RG sense; the asymptotic long wavelength properties are controlled by the disorder nonlinearity only. This is exactly analogous to the universality in the quenched disordered KPZ with long-range disorder. We show that as $\mu > 0$ is varied, both the quenched disordered KPZ and CKPZ equations can have a transition between a rough phase and a smooth phase. Last, the scaling exponents, which are calculated at the one-loop order, depend explicitly on γ and μ.

Beyond the specific results, we find the surprising generic conclusion that whenever quenched disorders are relevant (in the RG sense), the parameter γ enters into the expressions of the scaling exponents. Since γ can in principle vary continuously (between zero and infinity), so do the scaling exponents and hence does the universality class itself. We thus find *continuously varying universality*, induced by quenched disorder, in the two models that we considered. Furthermore, the existence of continuously varying universality appears to be quite robust: It exists with (CKPZ) or without (KPZ) a conservation law, so long as the quenched disorder itself remains relevant in the RG sense. We can relate this with the symmetry of the disorder distribution: γ is the parameter that determines the relative strengths of the transverse and longitudinal parts of the disorder variance. Thus, varying γ effectively means variation of the local alignment of $\mathbf{V}(\mathbf{q})$ with respect to $\mathbf{q}$. This continuous variation of the universality class is in fact more robust than our results perhaps imply. Since the variance of a quenched disordered vector field can generally be a combination of transverse and longitudinal parts, a dimensionless parameter like γ automatically arises, which remains a free parameter, continuously varying universal properties are generically expected so long as the quenched disorder remains relevant in the RG sense. These results may be tested by designing and simulating appropriate agent-based models coupled to a vector quenched disorder field with specified distributions. Do these results apply to annealed disorders as well? As shown in Appendix D, the CKPZ equations, when driven by vector fields with linear dynamics show this behavior. Preliminary results on the KPZ equation driven by an annealed disorder field also shows similar behavior (not shown here). This however comes with a caveat. An annealed field has a dynamics, which is not necessarily linear in general. We have assumed a linear dynamics for the annealed field only for simplicity. In general nonlinear terms should be present, which may or may not be relevant in

the RG sense. If it is relevant, then there is a possibility the dynamics of the annealed disorder field is renormalized, and that a parameter equivalent to γ may acquire specific RG fixed point value(s), instead of being a free, continuously varying parameter. Thus, it is possible that the resulting universality class of the height field (or in general a dynamical field driven by the annealed disorder) will *not* vary continuously. However, in the event the nonlinear effects in the dynamics of the annealed field are irrelevant, we expect continuously varying universality class to follow, as we have already found in the CKPZ equation with annealed disorder. We therefore conclude that, the existence of continuously varying universality classes with a vector quench disorder field is likely to be more generic than its annealed counterparts. Lastly, we caution the reader that the continuously varying universality class observed with quenched disorder here does not hold for *any* kind of quenched disorder, even if the disorder is relevant in the RG sense. This is because, in order for this result to hold, there must a free dimensionless parameter like γ in the disorder distribution. Not all quench disorder distributions may allow this. For instance, there is no scope of this in the recent studies on quenched columnar disordered KPZ equation [17,18], since the disorder there is a scalar.

Our results may be verified by direct numerical simulations of the stochastically driven equations of motion, which may be conveniently done by using pseudospectral methods [9]. It would be interesting to develop equivalent quenched disordered agent-based lattice-gas models, in terms of a height field or a phase field, which may be studied by using Monte Carlo simulations and explore and validate the RG results above. We hope our studies will provide new impetus in these directions.

Apart from their obvious theoretical interests, our results have experimental implications as well. For instance, a possible physical origin of the (vector) quenched disorder is the underlying disordered substrates. The substrates, if not very carefully prepared, may have different patches, characterized by different values of the parameter γ. For sufficiently large patches, each such patch should be characterized by scaling exponents parametrized by γ. If the experimental measurements are done on a region that includes may such patches having different γ, then the measured correlation functions are not likely to show any clean scaling, but should rather display a broadening of the measured values of the scaling exponents, or a kind of smeared scaling behavior. We hope our studies here will provide further impetus to research along these lines in the future.

APPENDIX A: GENERATING FUNCTIONAL

The generating functional of the disordered KPZ or CKPZ equation has the form [30,34–36]

$$\mathbb{Z} = \int_{\mathbf{x},t} \mathcal{D}\hat{h}\mathcal{D}h\mathcal{D}V e^{-S[\hat{h},h,V]}. \tag{A1}$$

Here S is the *action functional* and it contains two parts: (i) harmonic (S_H), (ii) anharmonic (S_A). Field $\hat{h}(\mathbf{x},t)$ is the dynamic conjugate field of $h(\mathbf{x},t)$ [30].

We here write the down the explicit forms of the action functionals for the disordered KPZ and CKPZ equations.

1. Disordered KPZ equation

The action functional is constructed by using Eq. (12) and averaging over the Gaussian-distributed noise ξ_h. We get

$$S_H^{\text{KPZ}} = \int_{\mathbf{x},t} [-D_1 \hat{h}\hat{h} + \hat{h}(\partial_t - \nu_1 \nabla^2)h]$$
$$+ \int_{\mathbf{x},\mathbf{x}'} \frac{V_{i_x}V_{j_{x'}}}{4[D_T P_{ij} + D_L Q_{ij}]|x - x'|^{-\alpha}}, \tag{A2}$$

$$S_A^{\text{KPZ}} = \int_{\mathbf{x},t} -\hat{h}\left[\frac{\lambda_1}{2}(\nabla h)^2 + \kappa_1(\mathbf{V}.\nabla h)\right], \tag{A3}$$

where S_H^{KPZ} and S_A^{KPZ} are, respectively, the harmonic and anhamornic parts of the action functional.

2. Disordered CKPZ equation

The action functional is constructed by using Eq. (14) and then averaging over the Gaussian-distributed noise η_h. We get

$$S_H^{\text{CKPZ}} = \int_{\mathbf{x},t} [-D_2(-\nabla^2)\hat{h}\hat{h} + \hat{h}(\partial_t + \nu_2 \nabla^4)h]$$
$$+ \int_{\mathbf{x},\mathbf{x}'} \frac{V_{i_x}V_{j_{x'}}}{4[D_T P_{ij} + D_L Q_{ij}]|x - x'|^{-\alpha}}, \tag{A4}$$

$$S_A^{\text{CKPZ}} = \int_{\mathbf{x},t} -\hat{h}\left[\frac{\lambda_2}{2}\nabla^2(\nabla h)^2 + \kappa_2 \nabla^2(\mathbf{V}.\nabla h)\right], \tag{A5}$$

where S_H^{CKPZ} and S_H^{CKPZ} are the harmonic and anharmonic parts of the action functional.

APPENDIX B: HARMONIC THEORY

In this section, we consider the harmonic parts of the action functionals, which correspond to the linear parts of the underlying stochastically driven equations of motion.

1. Disordered KPZ equation

The propagator and correlator of h in the Fourier space can be obtained from action Eq. (A2). These are

$$\langle \hat{h}_{-\mathbf{k},-\omega}h_{\mathbf{k},\omega}\rangle = \frac{1}{-i\omega + \nu_1 k^2}, \tag{B1a}$$

$$\langle |h_{\mathbf{q},\omega}|^2\rangle = \frac{2D_1}{\omega^2 + \nu_1^2 k^4}. \tag{B1b}$$

We thus get dynamic exponent $z = 2$ at all dimensions. The equal-time correlator in real space

$$C(r) \equiv \langle [h(\mathbf{x},t) - h(\mathbf{x}',t)]^2\rangle$$
$$= 2\int \frac{d^d\mathbf{k}}{(2\pi)^d} \frac{D_1[1 - e^{i\mathbf{k}\cdot[\mathbf{x}-\mathbf{x}']}]}{\nu_1 k^2}, \tag{B2}$$

for large $r \equiv |\mathbf{x} - \mathbf{x}'|$. Following Eq. (1), we conclude that $\chi_h = \frac{2-d}{2}$. Therefore, $\chi_h = 1/2$ at 1D and $\chi_h = 0$ at 2D in the Gaussian theory, or in the linearized Eq. (12).

2. Disordered CKPZ equation

The bare propagator and correlator of h in Fourier space can be obtained from the harmonic part of action Eq. (A4). These are

$$\langle \hat{h}_{-\mathbf{k},-\omega} h_{\mathbf{k},\omega} \rangle = \frac{1}{-i\omega + \nu_2 k^4}, \qquad \text{(B3a)}$$

$$\langle |h_{\mathbf{q},\omega}|^2 \rangle = \frac{2D_2 k^2}{\omega^2 + \nu_2^2 k^8}. \qquad \text{(B3b)}$$

Here $z = 4$, and the equal-time correlator $C(r)$ for this case in real space can be defined similarly as Eq. (B2) which gives $\chi_h = \frac{2-d}{2}$. It means $\chi_h = 1/2$ at 1D and $\chi_h = 0$ at 2D in the Gaussian theory, or in the linearized Eq. (14).

APPENDIX C: DYNAMIC RENORMALIZATION GROUP (RG) METHOD

We have discussed above about the method of dynamic RG, so, here we present the intermediate details such as loop diagrams, rescaling, fluctuation corrections.

1. One-loop Feynman diagrams

We represent the bare two-point functions, the anharmonic terms or the "vertices" in the action functional and the fluctuation-corrections of the model parameters by the Feynman diagrams, as shown in Fig. 8. These diagrams are for both the disordered KPZ and CKPZ equations. However, their expressions differ depending upon the model in question.
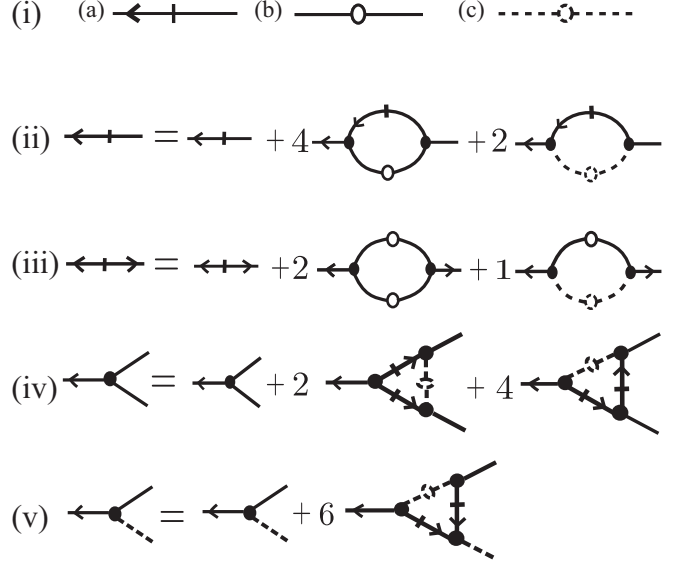

FIG. 8. (i) Bare two-point functions: (a) propagator, (b) correlator, (c) disorder correlator. Figures (ii)–(v) give the Feynman diagrams for the one-loop corrections in the theory; the one-loop diagrams have the same structure for in both the disordered KPZ and CKPZ equations, though their values differ (see text) . Figure (ii) give one-loop corrections to the diffusivity (ν_1 or ν_2), figure (iii) are for the noise strength (D_1 or D_2), figure (iv) are for the pure nonlinear terms (λ_1 or λ_2), and figure (v) correspond to the disordered nonlinear terms (κ_1 or κ_2). The number written before a Feynman diagram is the symmetry factor of the corresponding diagram.

a. Disordered KPZ equation

The fluctuation-corrections of the model parameters of the disordered KPZ Eq. (12) corresponding to the one-loop diagrams in Fig. 8 are given below:

$$\text{Fig. 8(ii): } \nu_1^< = \nu_1 \left[1 + \frac{2-d}{4d} \frac{\lambda_1^2 D_1}{\nu_1^3} \int_{\Lambda/b}^{\Lambda} \frac{d^d\mathbf{q}}{(2\pi)^d} \frac{1}{q^2} + \left(\frac{d-1}{d} \frac{2\kappa_1^2 D_T}{\nu_1^2} + \frac{\mu-d}{d} \frac{\kappa_1^2 D_L}{\nu_1^2} \right) \int_{\Lambda/b}^{\Lambda} \frac{d^d\mathbf{q}}{(2\pi)^d} \frac{1}{q^{2+\mu}} \right], \qquad \text{(C1a)}$$

$$\text{Fig. 8(iii): } D_1^< = D_1 \left[1 + \frac{\lambda_1^2 D_1}{4\nu_1^3} \int_{\Lambda/b}^{\Lambda} \frac{d^d\mathbf{q}}{(2\pi)^d} \frac{1}{q^2} + \frac{2\kappa_1^2 D_L}{\nu_1^2} \int_{\Lambda/b}^{\Lambda} \frac{d^d\mathbf{q}}{(2\pi)^d} \frac{1}{q^{2+\mu}} \right], \qquad \text{(C1b)}$$

$$\text{Fig. 8(iv): } \lambda_1^< = \lambda_1 \left[1 + \left(\frac{d-1}{d} \frac{2\kappa_1^2 D_T}{\nu_1^2} - \frac{2}{d} \frac{\kappa_1^2 D_L}{\nu_1^2} \right) \int_{\Lambda/b}^{\Lambda} \frac{d^d\mathbf{q}}{(2\pi)^d} \frac{1}{q^{2+\mu}} \right], \qquad \text{(C1c)}$$

$$\text{Fig. 8(v): } \kappa_1^< = \kappa_1 \left[1 - \frac{2}{d} \frac{\kappa_1^2 D_L}{\nu_1^2} \int_{\Lambda/b}^{\Lambda} \frac{d^d\mathbf{q}}{(2\pi)^d} \frac{1}{q^{2+\mu}} \right]. \qquad \text{(C1d)}$$

b. Disordered CKPZ equation

The fluctuation-corrections of the parameters in the disordered CKPZ Eq. (14) corresponding to the one-loop Feynman diagrams in Fig. 8 are given below:

$$\text{Fig. 8(ii): } \nu_2^< = \nu_2 \left[1 + \frac{4-d}{4d} \frac{\lambda_2^2 D_2}{\nu_2^3} \int_{\Lambda/b}^{\Lambda} \frac{d^d\mathbf{q}}{(2\pi)^d} \frac{1}{q^2} + \left(\frac{d-1}{d} \frac{2\kappa_2^2 D_T}{\nu_2^2} + \frac{\mu-d}{d} \frac{\kappa_2^2 D_L}{\nu_2^2} \right) \int_{\Lambda/b}^{\Lambda} \frac{d^d\mathbf{q}}{(2\pi)^d} \frac{1}{q^{2+\mu}} \right], \qquad \text{(C2a)}$$

$$\text{Fig. 8(iii): } D_2^< = D_2 + \text{subleading corrections,} \qquad \text{(C2b)}$$

$$\text{Fig. 8(iv): } \lambda_2^< = \lambda_2 \left[1 + \left(\frac{d-1}{d} \frac{2\kappa_2^2 D_T}{\nu_2^2} - \frac{2}{d} \frac{\kappa_2^2 D_L}{\nu_2^2} \right) \int_{\Lambda/b}^{\Lambda} \frac{d^d\mathbf{q}}{(2\pi)^d} \frac{1}{q^{2+\mu}} \right], \qquad \text{(C2c)}$$

$$\text{Fig. 8(v): } \kappa_2^< = \kappa_2 \left[1 - \frac{2}{d} \frac{\kappa_2^2 D_L}{\nu_2^2} \int_{\Lambda/b}^{\Lambda} \frac{d^d\mathbf{q}}{(2\pi)^d} \frac{1}{q^{2+\mu}} \right]. \qquad \text{(C2d)}$$

2. Rescaling

We rescale a Fourier wave vector and frequency as $\mathbf{k} \to b\mathbf{k}$ and $\omega \to b^z\omega$, equivalently in the real space $\mathbf{x} \to \mathbf{x}/b$, $t \to t/b^z$, where z is the dynamic exponent. The fields are accordingly rescaled as

$$h(\mathbf{k}, \omega) = \xi h(b\mathbf{k}, b^z\omega); \quad \hat{h}(\mathbf{k}, \omega) = \hat{\xi}\hat{h}(b\mathbf{k}, b^z\omega). \quad \text{(C3)}$$

Furthermore, $V_i(\mathbf{k}, \omega) = b^{z+\frac{d}{2}+\frac{\mu}{2}}V_i(b\mathbf{k}, b^z\omega)$, as obtained from Eq. (10).

a. Scaling of the parameters in the disordered KPZ equation

We set $\xi\hat{\xi} = b^{d+2z}$ by demanding the term in *action* Eq. (A2) $\int d^d\mathbf{k}\,d\omega\,\hat{h}h\omega$ does not scale under the rescaling of wave vectors and frequencies. Accordingly the model parameters scale as given below:

$$\nu_1' = \nu_1^< b^{z-2}, \quad D_1' = D_1^< b^{z-d-2\chi_h},$$

$$\lambda_1' = \lambda_1^< b^{z-2+\chi_h}, \quad \kappa_1' = \kappa_1^< b^{z-1+\frac{\mu}{2}-\frac{d}{2}},$$

$$D_L' = D_L^< = D_L, \quad D_T' = D_T^< = D_T. \quad \text{(C4)}$$

b. Scaling of the parameters in the disordered CKPZ equation

We set $\xi\hat{\xi} = b^{d+2z}$ by demanding the term in the action functional Eq. (A4) $\int d^d\mathbf{k}\,d\omega\,\hat{h}h\omega$ does not scale under the rescaling of wave vectors and frequencies. Accordingly the model parameters scale as given below:

$$\nu_2' = \nu_2^< b^{z-4}, \quad D_2' = D_2^< b^{z-d-2-2\chi_h},$$

$$\lambda_2' = \lambda_2^< b^{z-4+\chi_h}, \quad \kappa_2' = \kappa_2^< b^{z-3+\frac{\mu}{2}-\frac{d}{2}},$$

$$D_L' = D_L^< = D_L, \quad D_T' = D_T^< = D_T. \quad \text{(C5)}$$

APPENDIX D: ANNEALED DISORDER

We now briefly discuss what happens when the disorder is "annealed" instead of "quenched." This means the disorder is no longer frozen in time. At the simplest level, we model it by a time-dependent fluctuating vector field $\mathbf{U}(\mathbf{x}, t)$ that has zero mean and is assumed to be Gaussian distributed. If $\mathbf{U}$ is interpreted as a velocity field, then this is reminiscent of the well-known passive scalar turbulence problem [37–40]. The equation of motion of $\mathbf{U}$ is

$$\frac{\partial \mathbf{U}}{\partial t} = b\nabla^2\mathbf{U} + \mathbf{f}, \quad \text{(D1)}$$

where the noise $\mathbf{f}$ is zero-mean, Gaussian-distributed with a variance

$$\langle f_i(\mathbf{k}, \omega)f_j(\mathbf{k}', \omega')\rangle$$
$$= [2a_1P_{ij} + 2a_2Q_{ij}]k^{2-\mu}\delta^d(\mathbf{k} - \mathbf{k}')\delta(t - t'). \quad \text{(D2)}$$

Here, $\mu = d - \alpha$, as in the main text. Then the velocity autocorrelation function can be calculated exactly. In Fourier space it is

$$\langle U_i(\mathbf{k}, \omega)U_j(\mathbf{k}', \omega')\rangle$$
$$= \frac{2a_1P_{ij} + 2a_2Q_{ij}}{\omega^2 + b^2k^4}k^{2-\mu}\delta^d(\mathbf{k} + \mathbf{k}')\delta(\omega + \omega'), \quad \text{(D3)}$$

where $a_1/b = 2\tilde{D}_T$ and $a_2/b = 2\tilde{D}_L$. We are interested in the large b limit, with $\tilde{D}_L$ and $\tilde{D}_T$ being finite. In this limit, the annealed disorder autocorrelation in real space reduces to

$$\langle U_i(\mathbf{x}, t)U_j(\mathbf{x}', t')\rangle$$
$$= [2\tilde{D}_TP_{ij} + 2\tilde{D}_LQ_{ij}]|\mathbf{x} - \mathbf{x}'|^{-\alpha}\delta(t - t'). \quad \text{(D4)}$$

We briefly discuss the scaling properties of the disordered CKPZ equation with annealed disorder of the type defined above. The one-loop Feynman diagrams are identical to their quenched disorder counterparts. We focus on the one-loop diagrams which vanish in the absence of the annealed disorder.

Let us consider the last diagram in Fig. 8(ii) that originates from the disorder coupling κ_2 and corrects ν_2:

$$\int_{\mathbf{q}} \frac{(\mathbf{k} - \mathbf{q})_i(\mathbf{k} - \mathbf{q})^2 q^{2-\mu}(2a_1P_{ij} + 2a_2Q_{ij})_q}{bq^2[bq^2 + \nu_2(\mathbf{k} - \mathbf{q})^4]}, \quad \text{(D5)}$$

where $\mathbf{k}$ is an external wave vector and $\mathbf{q}$ is an internal wave vector of the one-loop diagram. Noise strength D_2 receives no relevant or diverging corrections.

In Fig. 8(iv) the triangle diagrams that originate from the disorder coupling κ_2 correct λ_2. They are:

$$\text{first triangle diagram} \sim \int_{\mathbf{q}} q^6q^{2-\mu}[2a_1P_{im} + 2a_2Q_{im}]$$

$$\left[\frac{1}{bq^2[\nu_2^2q^8 - b^2q^4]} - \frac{1}{\nu_2q^4[b^2q^4 - \nu_2q^8]}\right], \quad \text{(D6)}$$

$$\text{second triangle diagram}$$

$$\sim \int_{\mathbf{q}} \frac{q_mq_jq^4q^{2-\mu}[2a_1P_{im} + 2a_2Q_{im}]}{bq^2[bq^2 + \nu_2q^4]^2}. \quad \text{(D7)}$$

Similarly, the last diagram in Fig. 8(v), coming from the disorder vertex, corrects κ_2:

$$\int_{\mathbf{q}} \frac{q_mq_jq^4q^{2-\mu}[2a_1P_{im} + 2a_2Q_{im}]}{bq^2[bq^2 + \nu_2q^4]^2}. \quad \text{(D8)}$$

All the expressions of different one-loop diagrams given in Eqs. (D5)–(D8) are infrared divergent if $b \ll \nu_2q^2$ is satisfied. In fact, these corrections are same as in Eq. (C2). However, these diagrams give subleading corrections to the parameters in the opposite limit $b \gg \nu_2q^2$.

As the high wave-vector modes are being eliminated starting from $k = \Lambda$, the upper wave vector cutoff, there can be two situations: either ν_2k^2 dominates over b over a substantial range of (i.e., intermediate values of) wave vectors just below Λ, or b dominates over ν_2k^2 in the same wave-vector region. Noting that with ν_2 gaining positive corrections but b gets none, there can be two distinct possibilities.

(I) It is possible that as one eliminates the higher wave-vector modes, *before b* starts dominating, long enough RG time is spent, and the annealed-disordered CKPZ equation is *renormalized*. In this case, The corrections of parameters and corresponding flow equations are same as equations of Eq. (37). Therefore the result is identical to quenched disordered CKPZ equation. In this case, for even lower wave-vector regimes with $b \gg \nu_2k^2$, there are no new relevant fluctuation corrections to the model parameters. Hence, the same

universality as the quenched disordered CKPZ equation ensues, with a continuously varying parameter $\tilde{\gamma} \equiv \tilde{D}_T/\tilde{D}_L$ parametrizing the universality class.

(II) In the opposite case, not enough RG time is available to make ν_2 substantially renormalise, making b dominate over $\nu_2 k^2$ for low enough k. In this case, further more elimination from the disorder-dependent diagrams do not produce any relevant corrections to the parameters. However, the fluctuation corrections from the pure CKPZ nonlinear terms still survive, ultimately giving the scaling exponents of the pure CKPZ equation. In this case, naturally, there are no $\tilde{\gamma}$-dependence of the scaling exponents.

[1] U. C. Täuber, V. K. Akkineni, and J. E. Santos, Effects of Violating Detailed Balance on Critical Dynamics, Phys. Rev. Lett. **88**, 045702 (2002).

[2] B. Schmittmann and R. K. P. Zia, *Phase Transitions and Critical Phenomena*, edited by J. L. Lebowitz and C. Domb (Academic Press, London, 1972), Vol. 17.

[3] U. C. Täuber and E. Frey, Universality classes in the anisotropic Kardar-Parisi-Zhang model, Europhys. Lett. **59**, 655 (2002).

[4] M. E. Fisher, Scaling, universality and renormalization group theory, in *Critical Phenomena*, edited by F. J. W. Hahne (Springer, Berlin, 1983), pp. 1–139.

[5] P. M. Chaikin and T. C. Lubensky, *Principles of Condensed Matter Physics* (Cambridge University Press, Cambridge, UK, 2000), Vol. 1.

[6] P. C. Hohenberg and B. I. Halperin, Theory of dynamic critical phenomena, Rev. Mod. Phys. **49**, 435 (1977).

[7] A. Basu, Statistical properties of driven magnetohydrodynamic turbulence in three dimensions: Novel universality, Europhys. Lett. **65**, 505 (2004).

[8] A. Basu and E. Frey, Novel universality classes of coupled driven diffusive systems, Phys. Rev. E **69**, 015101(R) (2004).

[9] A. Basu and E. Frey, Scaling and universality in coupled driven diffusive models, J. Stat. Mech. (2009) P08013.

[10] A. Haldar, A. Sarkar, S. Chatterjee, and A. Basu, Can mobility induce orders in active oscillators on a substrate? arXiv:2104.10982.

[11] A. Haldar, A. Sarkar, S. Chatterjee, and A. Basu, Active mobile oscillators on a substrate: Density fluctuations and phase ordering, arXiv:2105.03919.

[12] U. Krey, On the critical dynamics of disordered spin systems, Z. Phys. B Condens. Matter **26**, 355 (1977).

[13] A. Weinrib and B. I. Halperin, Critical phenomena in systems with long-range-correlated quenched disorder, Phys. Rev. B **27**, 413 (1983).

[14] S. Mukherjee and A. Basu, Dynamic scaling in the quenched disordered classical *n*-vector model, Phys. Rev. Res. **2**, 033423 (2020).

[15] T. Banerjee and A. Basu, Thermal fluctuations and stiffening of symmetric heterogeneous fluid membranes, Phys. Rev. E **91**, 012119 (2015).

[16] T. Banerjee, N. Sarkar, and A. Basu, Phase transitions and order in two-dimensional generalized nonlinear σ models, Phys. Rev. E **92**, 062133 (2015).

[17] A. Haldar and A. Basu, Marching on a rugged landscape: Universality in disordered asymmetric exclusion processes, Phys. Rev. Res. **2**, 043073 (2020).

[18] A. Haldar, Universal properties of the Kardar-Parisi-Zhang equation with quenched columnar disorders, Phys. Rev. E **104**, 024109 (2021).

[19] S. Mukherjee, Conserved Kardar-Parisi-Zhang equation: Role of quenched disorder in determining universality, Phys. Rev. E **103**, 042102 (2021).

[20] A-L Barabási and H. E. Stanley, *Fractal Concepts in Surface Growth* (Cambridge University Press, Cambridge, UK, 1995).

[21] M. Kardar, G. Parisi, and Y.-C. Zhang, Dynamic Scaling of Growing Interfaces, Phys. Rev. Lett. **56**, 889 (1986).

[22] E. Altman, L. M. Sieberer, L. Chen, S. Diehl, and J. Toner, Two-Dimensional Superfluidity of Exciton Polaritons Requires Strong Anisotropy, Phys. Rev. X **5**, 011017 (2015).

[23] F. Cagnetta, M. R. Evans, and D. Marenduzzo, Kinetic roughening in active interfaces, EPJ Web Conf. **230**, 00001 (2020).

[24] E. Frey and U. C. Täuber, Two-loop renormalization-group analysis of the Burgers-Kardar-Parisi-Zhang equation, Phys. Rev. E **50**, 1024 (1994).

[25] T. Sun, H. Guo, and M. Grant, Dynamics of driven interfaces with a conservation law, Phys. Rev. A **40**, 6763 (1989).

[26] W. W. Mullins, Theory of thermal grooving, J. Appl. Phys. **28**, 333 (1957).

[27] C. Herring, Effect of change of scale on sintering phenomena, J. Appl. Phys. **21**, 301 (1950).

[28] H. K. Janssen, On Critical Exponents and the Renormalization of the Coupling Constant in Growth Models with Surface Diffusion, Phys. Rev. Lett. **78**, 1082 (1997).

[29] P. I. Kakin, M. A. Reiter, M. M. Tumakova, N. M. Gulitskiy, and N. V. Antonov, Stirred Kardar-Parisi-Zhang equation with quenched random noise: Emergence of induced nonlinearity, Universe **8**, 72 (2022).

[30] R. Bausch, H.-K. Janssen, and H. Wagner, Renormalized field theory of critical dynamics, Z. Phys. B Condens. Matter **24**, 113 (1976).

[31] U. C. Täuber, *Critical Dynamics: A Field Theory Approach to Equilibrium and Nonequilibrium Scaling Behavior* (Cambridge University Press, Cambridge, UK, 2014).

[32] N. D. Mermin and H. Wagner, Absence of Ferromagnetism or Antiferromagnetism in One- or Two-Dimensional Isotropic Heisenberg Models, Phys. Rev. Lett. **17**, 1133 (1966).

[33] V. Škultéty and J. Honkonen, Fixed-dimension renormalization group analysis of conserved surface roughening, Phys. Rev. E **104**, 024104 (2021).

[34] P. C. Martin, E. D. Siggia, and H. A. Rose, Statistical dynamics of classical systems, Phys. Rev. A **8**, 423 (1973).

[35] J. Zinn-Justin, *Quantum Field Theory and Critical Phenomena* (Clarendon Press, Oxford, UK, 2002), Vol. 113.

[36] C. DeDominicis and P. C. Martin, Energy spectra of certain randomly-stirred fluids, Phys. Rev. A **19**, 419 (1979).

[37] R. H. Kraichnan, Anomalous Scaling of a Randomly Advected Passive Scalar, Phys. Rev. Lett. **72**, 1016 (1994).

[38] L. Ts. Adzhemyan, N. V. Antonov, and A. N. Vasil'ev, Renormalization group, operator product expansion, and anomalous scaling in a model of advected passive scalar, Phys. Rev. E **58**, 1823 (1998).

[39] T. Banerjee and A. Basu, Perspectives on scaling and multiscaling in passive scalar turbulence, Phys. Rev. E **97**, 052124 (2018).

[40] S. Mukherjee and A. Basu, Scaling or multiscaling: Varieties of universality in a driven nonlinear model, Phys. Rev. E **103**, 032126 (2021).